Journal of Sedimentary Research

Journal of Sedimentary Research, 2021, v. 91, 913–928
Research Article
DOI: 10.2110/jsr.2020.153

GRAIN SIZE AND TRANSPORT BIASES IN AN EDIACARAN DETRITAL ZIRCON RECORD

MARJORIE D. CANTINE,*[1] JACOB B. SETERA,**[2] JILL A. VANTONGEREN,†[2] CHIZA MWINDE,[3] AND KRISTIN D. BERGMANN[1]
[1]Department of Earth, Atmospheric and Planetary Sciences, Massachusetts Institute of Technology, 77 Massachusetts Avenue, Cambridge, Massachusetts 02139, U.S.A.
[2]Department of Earth and Planetary Sciences, Rutgers University, Busch Campus, 610 Taylor Road, Piscataway, New Jersey 08854, U.S.A.
[3]Department of the Geophysical Sciences, University of Chicago, 5734 South Ellis Avenue, Chicago, Illinois 60637, U.S.A.
e-mail: mcantine@mit.edu

ABSTRACT: **Detrital-zircon records of provenance are used to reconstruct paleogeography, sediment sources, and tectonic configuration. Recognition of biases in detrital-zircon records that result from grain-size-dependent processes adds new complexity and caution to the interpretation of these records. We begin by investigating possible size-dependent biases that may affect interpretation of detrital-zircon provenance records in an idealized sedimentary system. Our modeling results show that settling and selective entrainment can differentially affect detrital-zircon spectra if an initial size variation between source zircon populations exists. We then consider a case study: a detrital-zircon record from Ediacaran to Terreneuvian strata of Death Valley, USA, with a focus on the Rainstorm Member of the Johnnie Formation. The detrital-zircon record of the Rainstorm Member shows that despite its unusual, heavy-mineral-rich character, the provenance of the unit is like other units in the succession. Size and density measurements of the grains of the deposit suggest that its enriched heavy-mineral suite is best explained through concentration by selective entrainment and winnowing. The relationship between detrital-zircon grain size and age for samples from the Johnnie Formation are consistent with grain-size influence on the interpretation of provenance, especially for large Grenville-age (1.0–1.2 Ga) zircons. Grain size can exert significant bias on a provenance interpretation and must be accounted for in provenance studies.**

INTRODUCTION

Detrital zircons are valuable tools in provenance studies. After zircon grains are eroded, transported, and redeposited, their original source regions are interpreted by matching their measured ages to source regions of known age. High-throughput dating by laser ablation has led to a rich literature in which detrital zircon grains constrain paleogeography, sediment provenance, and tectonics (e.g., Stevens et al. 2010; Cawood et al. 2012, 2013; Mackey et al. 2012; Gehrels 2014; Blum et al. 2017). Zircon makes up only a tiny fraction of most sedimentary rocks, but detrital-zircon provenance studies rely on the assumption that most or all samples from a stratigraphic unit will yield a similar interpretation of provenance and transport history of the component grains—but this is not always so.

Zircon's hardiness compared to other minerals (Smithson 1950; Carroll 1953; Morton and Hallsworth 2007) allows zircon grains to survive transport over long distances and multiple cycles of erosion, transport, and deposition compared to most other minerals (Fedo et al. 2003; Hawkesworth et al. 2009). This recalcitrance leads to difficulties in interpreting the record of provenance captured by detrital zircons because individual grains may correspond either with erosion of igneous or metamorphic primary sources (primary cycle grains) or erosion of sedimentary rocks with previously deposited detrital zircons (polycyclic grains). Analysis of grain cores and rims and comparison with other detrital minerals demonstrates the polycyclic character of some zircons (Hietpas et al. 2011a; Moecher et al. 2019; Flowerdew et al. 2020).

Source regions are not represented in the detrital-zircon record in proportion to the total volume of eroded sediment that they produce, but in proportion to their zircon fertility (Moecher and Samson 2006; Dickinson 2008; Hietpas et al. 2011b; Malusà et al. 2016; Spencer et al. 2018; Guo et al. 2020; Chew et al. 2020). Zircon fertility can span several orders of magnitude over regional spatial scales (Dickinson 2008; Malusà et al. 2016). In Laurentia, the Mesoproterozoic Grenville province (1.0–1.2 Ga) is particularly rich in zircon (Moecher and Samson 2006; Samson et al. 2018); these and other igneous rocks associated with the assembly of Rodinia have high Zr concentrations (Liu et al. 2017), and are likely over represented in the detrital-zircon record.

Zircon grains vary in size. Some evidence suggests that, in general, older zircons are finer and less variable in size than younger grains (Lawrence et al. 2011; Yang et al. 2012), although not all studies support this conclusion (Muhlbauer et al. 2017). Terrane-specific size differences may exist, too. In Laurentia, Grenville sources can produce very large (long axis on the order of 1000 μm) zircons; the *tips* of these zircons can be hundreds to thousands of times volumetrically larger than smaller zircons from neighboring terranes (Moecher and Samson 2006, their Fig. 5; Samson et al. 2018).

If detrital-zircon grain size varies by source region, then size-dependent sedimentary processes can systematically affect the apparent contribution

*Present Address: Institut für Geowissenschaften, Goethe-Universität, Altenhöferallee 1, 60438 Frankfurt am Main, Germany.
**Present Address: Department of Earth and Atmospheric Sciences, Cornell University, 112 Hollister Drive, Ithaca, New York 14853, U.S.A.
†Present Address: Department of Earth and Ocean Sciences, Tufts University, Lane Hall, Medford, Massachusetts 02155, U.S.A.

Published Online: September 2021

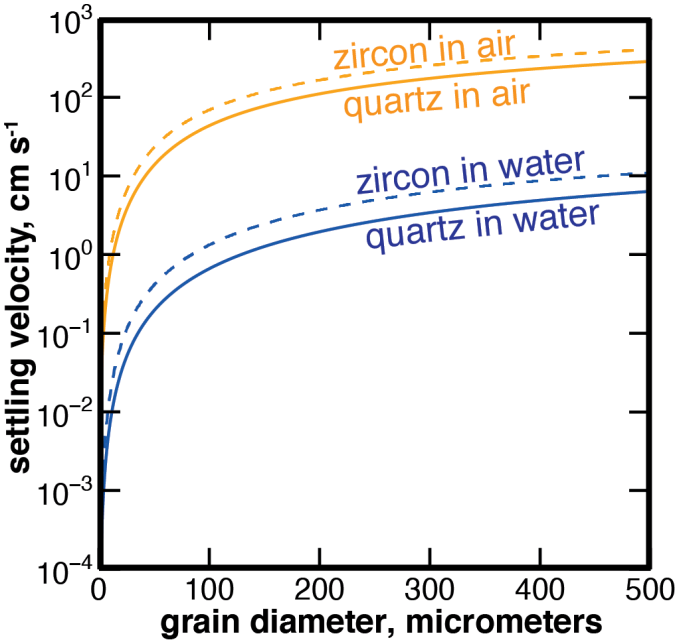

FIG. 1.—The settling velocities of quartz and zircon grains in water and air are shown as a function of grain diameter based on empirical measurements (Dietrich 1982; Bagheri and Bonadonna 2016; Raffaele et al. 2020). Solid lines are shown for quartz grains and dashed lines for zircon grains. Orange lines refer to sediment settling through air and blue to sediment falling through water. See text for explanation.

of sources. Studies of some modern systems (Lawrence et al. 2011; Hietpas et al. 2011b; Slama and Kosler 2012; Ibañez-Mejia et al. 2018; Malkowski et al. 2019) and ancient systems (Augustsson et al. 2018, 2019) show that grain size varies with source region and, in some cases, exerts control on detrital-zircon records. Studies of modern rivers even capture statistically significant variation in detrital-zircon populations over a single sand dune (Lawrence et al. 2011) or river profile (Ibañez-Mejia et al. 2018) due to the hydrodynamic sorting of sediment. In other successions, grain size does not appear to be a major control (Muhlbauer et al. 2017; Leary et al. 2020). Analytical procedures may add additional size-dependent biases (Gehrels 2000; Moecher and Samson 2006; Slama and Kosler 2012). The current best practice is to measure both zircon grain size and age, and then determine what, if any, relationship exists between them (Malusà and Garzanti 2019).

We explore how settling and selective entrainment may affect interpretation of provenance records using detrital zircon, first with a model of an idealized sedimentary system. We then investigate the role of grain size and sedimentary processes in shaping a detrital-zircon record from an Ediacaran to Terreneuvian sedimentary succession in Death Valley, USA, focusing on the Rainstorm Member of the Johnnie Formation.

Grain Size, Density, and Process in Clastic Deposits

Differences in density between zircon ($\rho = 4.65$ g/cm^3) and less dense minerals, like quartz ($\rho = 2.65$ g/cm^3), may be reflected in the different grain size of zircon and quartz grains deposited together. For sediment deposited by settling from suspension, grains with the same uniform settling velocity are hydraulically equivalent and will be deposited together (Rubey 1933). Grain size and density are the most important variables in determining settling velocity for subspherical grains (Dietrich 1982). Increases in grain density are compensated by decreases in grain diameter, so smaller zircon grains settle with larger quartz grains.

Empirical relationships derived from meta-analyses of settling experiments (e.g., Clift and Gauvin 1971; Gibbs et al. 1971; Dietrich 1982; Cheng 1997; Ferguson and Church 2004; Bagheri and Bonadonna 2016; Raffaele et al. 2020) capture the combined effects of turbulence and fluid viscosity on settling velocity in fluids of different properties, like air and water (Fig. 1; Supplemental Material). Relative to a constant quartz grain size, zircon grains deposited by settling in air will be larger than zircon grains deposited by settling in water (Fig. 1). This difference is driven by the greater contrast between the submerged density of quartz and zircon grains in water than in air. Aeolian settling deposits are thus biased towards larger zircon grains relative to subaqueous settling deposits, all else held equal (Figs. 1, 2; Supplemental Material). The textural characteristics of sand, including size distribution and relative sizes of heavy and light mineral grains, can distinguish between river, beach, and aeolian dune sands (Friedman 1961).

For sediment transported and deposited in bedload, processes in addition to settling control the size distribution and abundance of heavy-mineral and quartz grains (Friedman 1961; Lowright et al. 1972; Slingerland 1977; Komar and Wang 1984; Slingerland 1984; Slingerland and Smith 1986; Komar et al. 1989; Komar 2007). Downstream fining, or decreasing grain size with increased transport distance, is recorded in modern rivers and dune fields. Both abrasion of particles (Kodama 1994; Lewin and Brewer 2002) and selective deposition and transport (Paola et al. 1992; Ferguson et al. 1996; Gasparini et al. 1999) contribute to this phenomenon. Given zircon's hardiness, abrasion is likely less important than for most other grains, but zircon grains can still be abraded and broken. Selective deposition of particles could impact the detrital-zircon record of a sedimentary system, with larger grains deposited in coarser, more proximal settings, and finer grains in more distal locations.

Grain shape and size control the selective entrainment of grains (McIntyre 1959; Lowright et al. 1972; Slingerland 1977, 1984; Komar and Li 1988; Komar et al. 1989). At one extreme, coarse, light grains, which project into the flow and have relatively small pivot angles, are selectively entrained (Fig. 2). The resulting deposit becomes both heavy-mineral enriched and well sorted, as in some placer deposits in which heavy-mineral grains and quartz grains are close in size (Slingerland 1977). We refer to this type of sediment as an *equal-sizes* deposit (Fig. 2, Supplemental Material). At the other extreme, the shielding of small, dense minerals by larger, less dense grains on the bed results in deposits with very small heavy-mineral grains relative to quartz grains (Rittenhouse 1943; McIntyre 1959; Briggs 1965; Grigg and Rathbun 1965; Hand 1967; Lowright et al. 1972; Slingerland 1977; Steidtmann and Haywood 1982; Komar and Wang 1984; Komar and Li 1988; Komar 2007). We refer to this as the *grain-shielding* case (Fig. 2, Supplemental Material). These processes produce a poorly sorted deposit in which small, denser grains have slower settling velocities relative to larger, less dense grains (Fig. 2, Supplemental Material). Garzanti et al. (2009) describe an aeolian sand with small heavy minerals relative to quartz grains. We interpret this deposit to have formed by grain shielding during transport by traction and saltation, as described in another aeolian setting by Steidtmann and Haywood (1982). We use the grain-size-to-density parameterization of Garzanti et al. (2009) to describe it.

Other processes may impact the detrital-zircon record of a sediment sample but are not considered in this study. For example, variations in flow over bedforms like ripples and dunes can lead to preferential deposition of heavy minerals near crests (McQuivey and Keefer 1969; Brady and Jobson 1973). Localized deposition of heavy minerals can also occur in response to flow changes around larger geomorphic features like bars or river confluences (Smith and Beukes 1983; Day and Fletcher 1989). Shear sorting during transport produces density-stratified deposits in which dispersive equivalence controls the sizes of distribution of deposits (Emery and Stevenson 1950; Clifton 1969; Sallenger 1979).

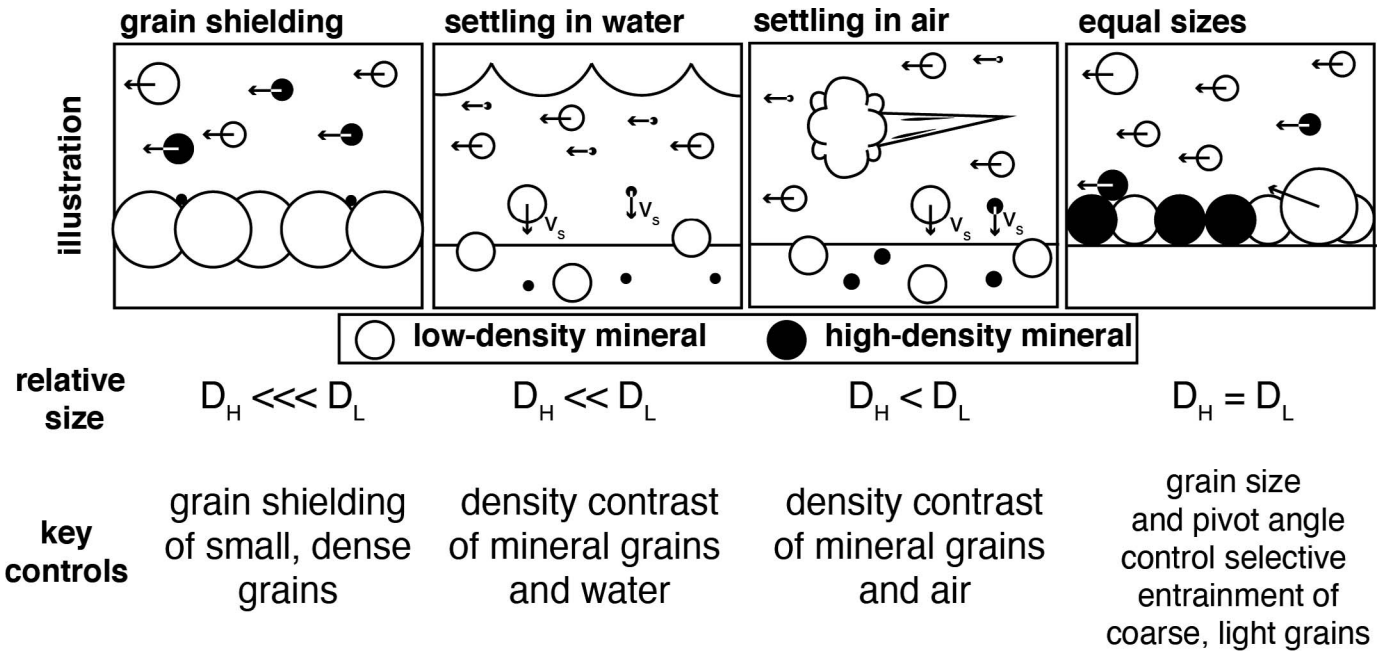

FIG. 2.—Illustration of the four scenarios explored in this model and their consequences for the relative sizes of heavy and light mineral grains. In the first scenario, grain shielding of small, heavy-mineral grains by larger, light-mineral grains yields a deposit with very small heavy-mineral grains relative to light mineral grains. In the middle scenarios, the density contrast between air or water and the light- or heavy-mineral grains produces a deposit with smaller heavy-mineral grains than light-mineral grains; the greater density contrast in water results in a greater size difference. In the final scenario, selective entrainment of large grains that project above the bed results in a well-sorted, heavy-mineral-rich deposit in which heavy and light mineral grains are the same size.

We apply these insights in the context of an Ediacaran–Terreneuvian detrital zircon record from Death Valley, with a focus on the Ediacaran Rainstorm Member of the Johnnie Formation. Given the reported large size difference between Grenville zircon grains and those from other terranes (Moecher and Samson 2006; Samson et al. 2018), we hypothesized that fine-grained samples would have a smaller Grenville-sourced component than coarser samples. Because grain size decreases with transport distance, we hypothesize that distal deposits would have smaller Grenville components compared to proximal deposits. Evidence for extensive winnowing and reworking of Rainstorm Member sediment (Summa 1993; Pruss et al. 2008; Bergmann et al. 2013) suggests that grain–bed interactions, which drive selective entrainment, were more important than settling during deposition of the unit, and impacted the detrital-zircon record of this unit.

GEOLOGICAL CONTEXT

The westward-thickening, Ediacaran to Terreneuvian strata of Death Valley record deposition in a mixed siliciclastic–carbonate, rift-to-passive margin succession which includes the Johnnie Formation, Stirling Quartzite, and Wood Canyon Formation (Fig. 3) (Stewart 1970; Summa 1993; Fedo and Cooper 2001; Corsetti and Kaufman 2003; Clapham and Corsetti 2005; Verdel et al. 2011; Schoenborn et al. 2012). Previous studies examined detrital-zircon age spectra through the succession and showed varying contributions from the Grenville, Yavapai–Matzatzal, and mid-continent regions, as well as smaller contribution from Archean sources (Stewart et al. 2001; Verdel et al. 2011; Schoenborn et al. 2012; Muhlbauer et al. 2017).

The Rainstorm Member

The uppermost member of the Johnnie Formation is the Rainstorm Member, a shallow marine, storm-dominated, mixed siliciclastic–carbonate unit with unusual sedimentological, mineralogical, and geochemical features (Stewart 1970; Summa 1993; Corsetti and Kaufman 2003; Corsetti et al. 2004; Kaufman et al. 2007; Pruss et al. 2008; Bergmann et al. 2011, 2013). In the Rainstorm Member, siltstone and sandstone are interbedded with pink and gray limestone containing ooid grainstone, intraclast and edgewise conglomerate, and, locally, crystal fans (Fig. 4) (Stewart 1970; Summa 1993; Corsetti et al. 2004; Pruss et al. 2008; Bergmann et al. 2013).

Near its base, the Rainstorm Member is interpreted as a highstand deposit with an initial marine transgression recorded by the time-transgressive Johnnie Oolite (Stewart 1970; Summa 1993; Bergmann et al. 2011) Hummocky cross-stratification and planar lamination are abundant throughout (Summa 1993). Upsection, the Rainstorm Member includes an incised-valley fill with a basal incision surface that, in some locations, erodes the lower Rainstorm completely (Stewart 1970; Summa 1993; Corsetti and Kaufman 2003; Clapham and Corsetti 2005; Trower and Grotzinger 2010; Verdel et al. 2011). This incision surface is interpreted either as tectonic (Summa 1993; Clapham and Corsetti 2005) or glacioeustatic (Christie-Blick and Levy 1989; Abolins et al. 2000; Witkosky and Wernicke 2018) in origin.

In the southern Nopah Range, Rainstorm limestone beds contain approximately 1-cm-tall carbonate crystal fans neomorphosed to calcite from primary aragonite (Summa 1993; Corsetti et al. 2004; Pruss et al. 2008; Bergmann et al. 2013) (Fig. 4). These strata are also heavy-mineral rich and include detrital zircon, titanium oxide, and hematite grains (Bergmann et al. 2013). Crystal fans nucleated on heavy-mineral-rich horizons, and sediment infill between crystal-fan blades includes detrital heavy minerals as well as ooids and intraclasts (Fig. 4) (Summa 1993; Pruss et al. 2008; Bergmann et al. 2013). Like other examples of crystal fans through Earth history (Bergmann et al. 2013), Rainstorm crystal fans developed during a period of maximum flooding and low background sedimentation rate (Summa 1993; Corsetti et al. 2004; Pruss et al. 2008; Bergmann et al. 2013). Most Rainstorm crystal-fan layers remain *in situ*,

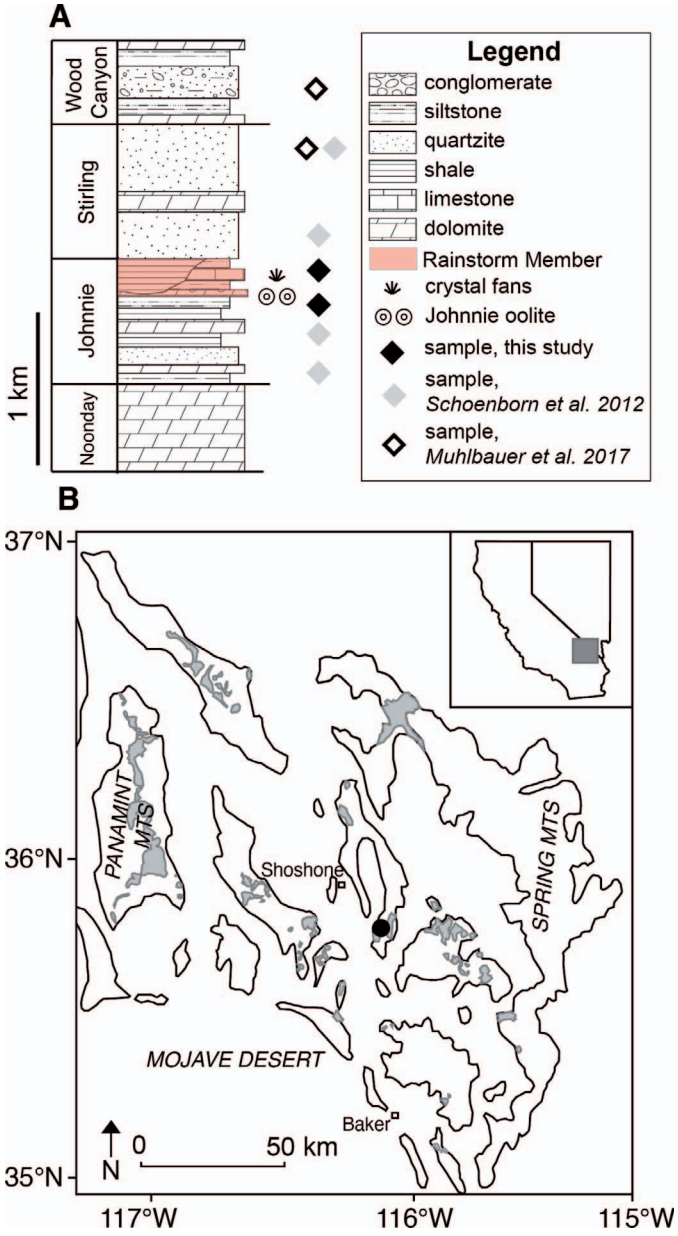

FIG. 3.—**A)** The Ediacaran to Terreneuvian succession of Death Valley, Nevada and California, USA, is shown. The lowermost Noonday Dolomite is considered earliest Ediacaran near its base (Prave 1999; Petterson et al. 2011) and the Wood Canyon Formation straddles the Ediacaran–Cambrian boundary (Corsetti and Hagadorn 2000). The approximate stratigraphic position of samples from this study and previous studies (Schoenborn et al. 2012; Muhlbauer et al. 2017) are shown as diamonds. The Rainstorm Member, the particular focus of this study, is highlighted in pink. **B)** The areal extent of the Johnnie Formation, of which the Rainstorm Member is the uppermost unit, is shown in gray. The southern Nopah Range, where Rainstorm samples were collected for this study, is marked with a black dot. Modified after Bergmann et al. (2011), their Figure 2.

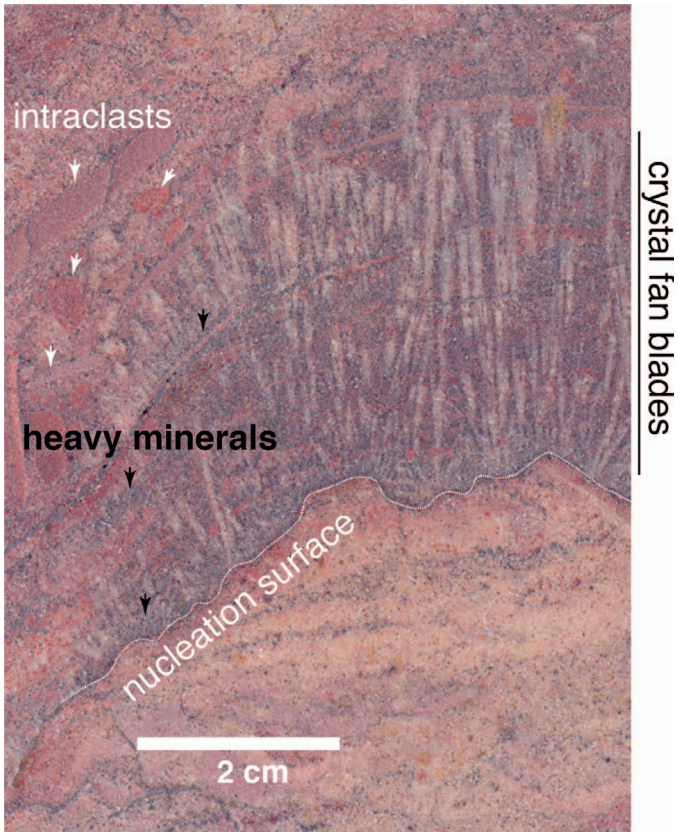

FIG. 4.—A representative crystal-fan-bearing limestone bed from the Rainstorm Member is shown in a cut and polished slab. Formerly aragonite (Pruss et al. 2008) crystal fans nucleate on a scoured seafloor surface, traced with a dotted white line. Heavy-mineral-enriched clastic grains are abundant in the sample, visible as dark gray to black zones; a few examples are indicated with black arrowheads. Carbonate intraclasts are also abundant, and a few examples are indicated with white arrowheads. Modified after Bergmann et al. (2013), their Figure 5A.

and their small size and delicate shape suggests that they formed in relatively quiet conditions (Summa 1993; Pruss et al. 2008) although crystal-fan intraclasts (Bergmann et al. 2013, their Fig. 5) show that some crystal fans were disrupted and reworked during high-energy events.

The Rainstorm Member also hosts the nadir of an extremely negative carbon isotope excursion, with values as low as –12‰ $\delta^{13}C_{VPDB}$ (Corsetti and Kaufman 2003; Kaufman et al. 2007; Verdel et al. 2011). This excursion has been correlated with the global Shuram carbon isotope excursion (c. 574 to 567 Ma, Rooney et al. 2020) on the basis of its magnitude; asymmetric onset and recovery; position within middle Ediacaran strata; and estimated duration (Corsetti and Kaufman 2003; Kaufman et al. 2007; Bergmann et al. 2011; Grotzinger et al. 2011; Verdel et al. 2011; Minguez et al. 2015; Witkosky and Wernicke 2018; Canfield et al. 2020; Matthews et al. 2020; Rooney et al. 2020).

Based on Nd isotope data, Schoenborn et al. (2012) suggested that the provenance of the Rainstorm Member was primarily the Yavapai and Matzatzal provinces. However, Schoenborn et al. (2012) note that these data do not definitively distinguish between this scenario and one in which the sources include the Mojave and/or Yavapai–Matzatzal provinces and the Grenville province.

MATERIALS AND METHODS

Grain Mixing Model

To explore the influence of grain size, settling, and selective entrainment on detrital zircon records, we built a numerical model that generates synthetic quartz and zircon grain data for two source regions with defined age and size characteristics (Figs. 2, 5; Table 1, Supplemental Material. See Supplemental Material for information on the code used for this analysis). Quartz grains of all sizes are generated, but zircon grains have a characteristic size distribution.

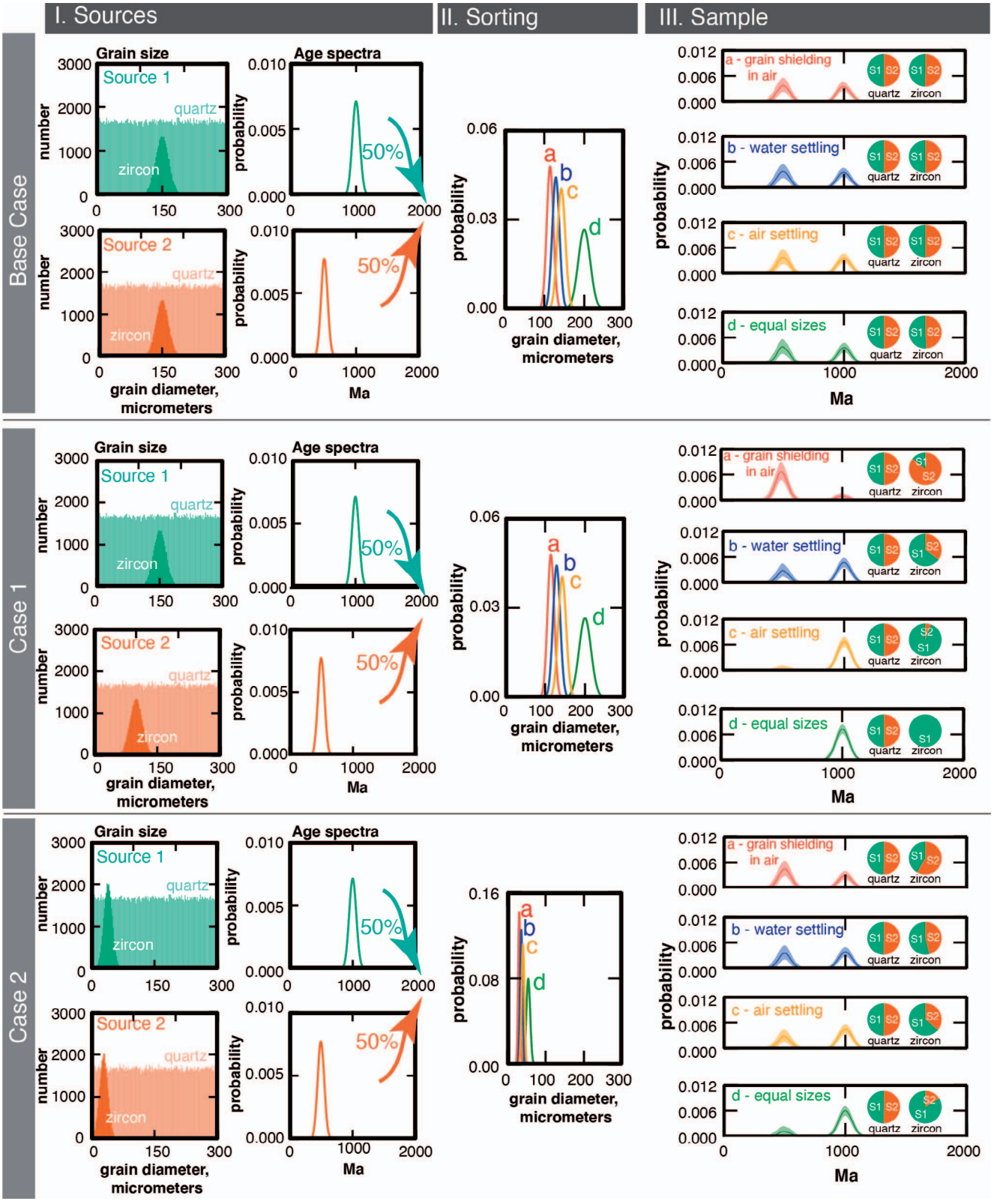

FIG. 5.—The grain-size and age spectra of two source populations containing both quartz and zircon grains are shown in column I. These populations are mixed together. Column II shows four different size distributions, which correspond to four different depositional scenarios explored in this work. All are relative to a model-defined quartz grain size. In the equal-sizes scenario, the deposited quartz and zircon grains have the same average size. In the two settling cases, the probability of zircon grains being deposited with a particular quartz grain size is determined by their settling velocity in either water (Dietrich 1982) or air (Bagheri and Bonadonna 2016; Raffaele et al. 2020). In the grain-shielding scenario, we use observations from a modern aeolian dune described in Garzanti et al. (2009) to define the probability of deposition. (See Supplemental Material for equations). For each scenario, 100 quartz and 100 zircon grains are selected 10,000 times using these probability distributions. Column III shows the resulting synthetic spectra with a 95% confidence interval envelope and the proportions of grains from different sources. This analysis is performed for each of three cases: a base case, in which grain sizes are identical between source regions, and two cases in which zircon grain size differs between source regions.

Each grain is randomly assigned an age and grain size based on defined parameters for its source region, as well as a 2σ age uncertainty of 5% of the grain's age, mirroring the uncertainty associated with laser-ablation $^{206}Pb/^{207}Pb$ age measurements. The source regions are mixed in a defined ratio. From the combined pool, 100 grains of quartz and zircon are then randomly selected, representing the deposition of grains. For quartz grains, the probability of being deposited is determined by a defined mean grain size and standard deviation. The size-dependent probability of deposition for zircon grains varies depending on scenario, as described below. After deposition, an age spectrum of zircons is determined. Synthetic spectra are generated this way 10,000 times.

The model considers four possible scenarios (Fig. 2, Table 1, Supplemental Material). In one end member, the equal-sizes scenario, the zircons deposited have the same size as the quartz grains deposited, as in well-sorted, heavy-mineral-rich deposits, like placer sand, that form under specific conditions of flow and bed roughness (Slingerland 1977). The other end-member relationship, the grain-shielding scenario, uses observations reported by Garzanti et al. (2009) from a modern aeolian sand to determine the size difference between deposited quartz and zircon grains. Intermediate to these two end members are scenarios in which deposited zircon grains have the same settling velocity as quartz grains in both water (Dietrich 1982) and air (Bagheri and Bonadonna 2016; Raffaele et al. 2020) (Fig. 5, column II).

In all cases described here, the two source regions are mixed in a 1:1 ratio, and the zircon fertility, or ratio of quartz grains to zircon grains in each region, is held constant at 10:1, an illustrative value chosen to maintain the speed of the model. Geological measurements of zircon fertility are smaller, typically $<$ 100 ppm (Malusà et al. 2016); we use the 10:1 ratio to maintain a reasonable model runtime. Parameters that vary between cases are given in Table 1.

Base Case.—This case mixes two source regions, identical except for the ages associated with the source regions. Grains from source 1 have a population age of 1000 Myr with a standard deviation of 50 Myr; source 2 grains have a population age of 500 Myr with a standard deviation of 50 Myr. The sizes of quartz grains from both source regions are uniformly distributed between 0 and 300 μm. Zircon from both regions has a mean grain size of 150 μm with a standard deviation of 15 μm. The deposited quartz sediment has a mean grain size of 200 μm with a standard deviation of 15 μm.

Case 1.—This case is identical to the base case, with the single change that zircons from source 2 are smaller than zircons from source 1. Source 2 zircons have a mean grain size of 100 μm with a standard deviation of 15 μm.

Case 2.—This case explores behavior in finer-grained sediment. In this case, both source 1 and 2 quartz grains have a mean grain size of 80 μm with a standard deviation of 15 μm. Source 1 zircons have a mean grain size of 40 μm with a standard deviation of 10 μm; source 2 zircons have a mean grain size of 30 μm with a standard deviation of 10 μm. Deposited quartz has a mean grain size of 55 μm with a standard deviation of 5 μm.

Change along a Transport Path.—In addition to these cases, we explore how changes along the transport path of sediment could influence the interpretation of provenance. We investigate an idealized system with three detrital-zircon source populations that systematically vary in size and age. We define four deposits along the sediment-transport path: a proximal medium-grained sand from a subaqueous dune affected by grain shielding; a proximal medium-grained overbank sand deposited by settling through water; a distal fine-grained overbank sand deposited by settling through water; and a distal very fine-grained sand formed by aeolian reworking of sediment that is affected by grain shielding. These deposits fine downstream. We use the same approach as above to calculate the corresponding detrital-zircon size associated with each deposit (Supplemental Material) and generate synthetic spectra for each.

Rainstorm Sample Characterization

Samples were collected in the southern Nopah Range (see Supplement for locations), including a very fine-grained quartz sandstone below the Johnnie Oolite and crystal-fan-bearing, heavy-mineral-rich strata in the Rainstorm Member. Standard zircon separation procedures, including magnetic and heavy-liquid separation, were used for the sandstone sample. The crystal-fan-bearing samples were dissolved in 20% hydrochloric acid to remove carbonate. After dissolution, the heavy-mineral-rich residue was separated following standard zircon separation procedures. Before analysis, zircons were mounted, polished, and imaged by either cathodoluminescence or light microscope.

Geochronology.—U-Pb ages of zircons were obtained via LA-ICP-MS using a Photon Machines 193 nm laser ablation system coupled to a Thermo iCapQc^{TM} mass spectrometer at Rutgers University. Laser power was set at 50% power and a 10 Hz rep rate, resulting in a fluence of 4.25 J/cm^2 at the surface of the zircon. The laser spot size was 20 μm. This small spot size was used to minimize sample destruction during analysis, so that any young, concordant grains could be dated with high-resolution U/Pb thermal-ionization mass spectrometry (TIMS). Ablated material was carried to the plasma via helium gas at a total flow rate of 0.8 LPM. For each analysis, the iCapQc^{TM} was set up to acquire data for $\sim$ 220 sweeps with a 10 millisecond per isotope dwell time. Laser firing and ablation lasted for 30 seconds during each analysis, whereas gas blanks were measured for approximately 20 seconds immediately before each zircon analysis using the same instrumental conditions (without firing the laser). Washout time between each analysis and the start of the next background was approximately 1 minute. Data processing was performed primarily using the Iolite software package with $^{206}Pb/^{207}Pb$ ages calculated using ISOPLOT (Ludwig 2003). $^{206}Pb/^{207}Pb$ ages are used in order to make direct comparison to the results of Schoenborn et al. (2012). The use of $^{206}Pb/^{238}U$ ages rather than $^{206}Pb/^{238}U$ ages would yield the same conclusions.

Grains were screened for concordance between their $^{206}Pb/^{238}U$ and $^{207}Pb/^{206}Pb$ ages, and only those with $<$ 10% discordance were included in the analysis. Ages presented are $^{207}Pb/^{206}Pb$ ages.

Detrital zircon age spectra for the lower and middle Johnnie Formation and the Stirling Quartzite were previously published in Schoenborn et al. (2012). Spectra for the upper Stirling Quartzite and Wood Canyon Formation were published in Muhlbauer et al. (2017).

Zircon Size Determination.—The long and short axis of each grain from the Rainstorm Member was measured, either by cathodoluminescence (CL) imaging or with a light microscope. Cathodoluminescence images of grains from the lower and middle Johnnie Formation and lower and upper Stirling Quartzite (Schoenborn et al. 2012) are available in the appendices of Schoenborn (2010). Long axes for upper Stirling Quartzite and Wood Canyon Formation grains were previously published in Muhlbauer et al. (2017). Only concordant grains for which a grain size could be determined are included in this study.

Previous detrital-zircon grain size studies have used either the equivalent spherical diameter (ESD) of zircon grains (e.g., Lawrence et al. 2011) or the long axis of grains (e.g., Muhlbauer et al. 2017). The ESD better accounts for the hydrodynamic characteristics of a zircon grain than a measurement of its long axis alone (Garzanti et al. 2008; Lawrence et al. 2011). However, data easily available for all grains was limited to measurements of long axes. This study uses the long axes of detrital

zircons to quantify their grain size, although the size trends described in this study are consistent using ESD for the subpopulation of samples for which ESD can also be calculated.

Size and Density of Clastic Material from Crystal Fans.—A sample of heavy-mineral-rich, crystal-fan-bearing carbonate from the Rainstorm Member was dissolved, as described above, in 20% hydrochloric acid. The heavy-mineral-rich residue was separated into heavy and light fractions using the heavy liquid methylene iodide ($\rho = 3.32$ g/cm^3). The greater part, by volume and by mass, separated into the heavy fraction (Table 2). The fractions' densities were determined through volume displacement. The intermediate axis lengths of the heavy and light fractions were determined using a laser particle-size analyzer at the University of Oklahoma.

Modeling Size–Age Relationships in the Ediacaran–Terreneuvian Death Valley Succession

To explore the signature of grain size in data from this succession, we pooled all measured age and grain-size data for zircon grains from these units. We defined four size distributions, each corresponding to the size distributions of zircon grains from a particular unit: 69 ± 16 μm (1 sd; Rainstorm crystal fans); 89 ± 21 μm (1 sd; Rainstorm sandstone); 124 ± 32 μm (1 sd; Lower Johnnie Formation), and 154 ± 50 μm (1 sd; Wood Canyon Formation). Then, these size distributions were used to randomly select 60 grains from the pool of all zircons, a process repeated 10,000 times. The resulting age spectra from each subset of 60 grains was determined (see Supplemental Material section for the code used for this analysis).

RESULTS

Size Mixing Model

Our results illustrate that size-dependent processes, together with systematic initial grain size–age variation, can result in very different measured detrital-zircon spectra for deposits with a shared provenance (Fig. 5). For each case, the age and size distribution of quartz and zircon grains from two source regions are calculated (Fig. 5, column I). The two sources are combined. The probability of deposition for each grain is determined under various scenarios, described above. One hundred zircon grains and 100 quartz grains are selected from each pool according to the probability of deposition. This selection is repeated 10,000 times, and the median and 95% confidence interval of all results are determined (column III). The proportion of quartz and zircon grains deposited from each source region across all runs is calculated (Fig. 5, column III).

Base Case.—Results from the base case provide a point of comparison: all parameters, except for the age of detrital-zircon grains, are consistent between the two sources. The measured age spectra for all scenarios accurately record the 1:1 sediment input for both quartz and zircon grains with no change across the four modeled deposits.

With grain size held equal between the two sources, the resulting detrital-zircon spectra match the quartz sources well. On average, they are a faithful record of sediment source across each case explored here, although randomness within individual spectra still lead to variation in interpretation. Some of the parameters held constant in this simulation—including consistent zircon fertility and constant grain size between source regions—may often not be equal between source regions in real settings.

Case 1.—Case 1 is identical to the base case except that source 2 zircons are smaller than source 1 grains. The resulting synthetic deposits show a range of spectra with shifting source 1 and source 2 inputs based on grain size. The grain-shielding scenario shows an average of 85% source 2 input, whereas the equal-sizes scenario shows nearly 100% source 1 input. Deposits formed from the settling of grains through air and water both show a majority of source 1 (larger) grains, but with differences in the proportion. The case shown for settling through air has 6% source 2 grains on average and the case shown for settling through water has 35% source 2 grains on average.

Across all modeled deposits, deposited quartz grains are split evenly between the source regions. In this case, an initial difference in the average detrital-zircon size of two populations results in a wide range of age spectra. The synthetic spectra range from mostly source 2 to all source 1, depending on the grain-size variation of each deposit. The interpreted provenance of these samples, if based only on measurements of zircon grains, does not always capture the actual contribution of each source region, even though both source areas contributed equal amounts of quartz sediment.

Case 2.—Case 2 explores process-dependent grain-size shifts at smaller quartz and zircon grain sizes than case 1. Deposits show a range of spectra with variable contributions from sources 1 and 2. At one extreme, the grain-shielding scenario contains a slight majority of source 2 grains. The other three transport cases show more source 1 grains than source 2 grains in varying proportions. As in case 1, an initial difference between detrital-zircon populations results in a range of spectra across the cases studied, and the interpreted provenance of samples, if based only on measurements of zircon grains, do not necessarily capture the actual sediment contributions of each source region.

These results suggest that settling and selective entrainment can impart differential signatures to detrital-zircon records if systematic differences in grain size between samples exist. The properties of the transport medium, as well as grain–grain and grain–bed interactions, play a role in defining that signature.

Change along a Transport Path.—In an idealized system where systematic differences in size and age between zircon populations exist, changes in grain size and the influence of settling and selective entrainment lead to different detrital-zircon age spectra along a transport path (Fig. 6). These records also reflect different influences from settling and grain shielding. Grain size varies along the transport path of sediment. Drawing from the same initial source populations but changing grain size and the influence of settling and selective entrainment, we demonstrate that the detrital-zircon age spectra of samples could vary along a transport path (Fig. 6), potentially leading to interpreted changes in provenance better explained by variability in grain size and transport process.

Rainstorm Sample Characterization

Geochronology.—Age spectra from combined new and previously published (Schoenborn et al. 2012; Muhlbauer et al. 2017) zircon ages, as well as grain-size measurements (Figs. 7, 8), show four primary subpopulations (~ 1.0–1.2 Ga; ~ 1.3–1.5 Ga; ~ 1.6–1.9 Ga; and > 2.0 Ga). These subpopulations are interpreted to have their origin in the Grenville orogen (~ 1.0–1.2 Ga), the midcontinent (~ 1.3–1.5 Ga), the Yavapai–Mazatzal or Central Plains regions (~ 1.6–1.9), and older cratonic sources (> 2.0 Ga) (Dickinson and Gehrels 2009). The relative contribution of Grenville-age material waxes and wanes through the section. This peak is absent or minimal in the Lower Johnnie, Rainstorm crystal fans, and upper Stirling Quartzite. It is particularly pronounced in the Wood Canyon Formation, as others have noted (Stewart et al. 2001; Muhlbauer et al. 2017).

Zircon Size Characterization.—We document that Grenville-age grains are, on average, larger than their Paleoproterozoic counterparts (Fig. 8). Zircon grains from Rainstorm crystal-fan beds are finer than other

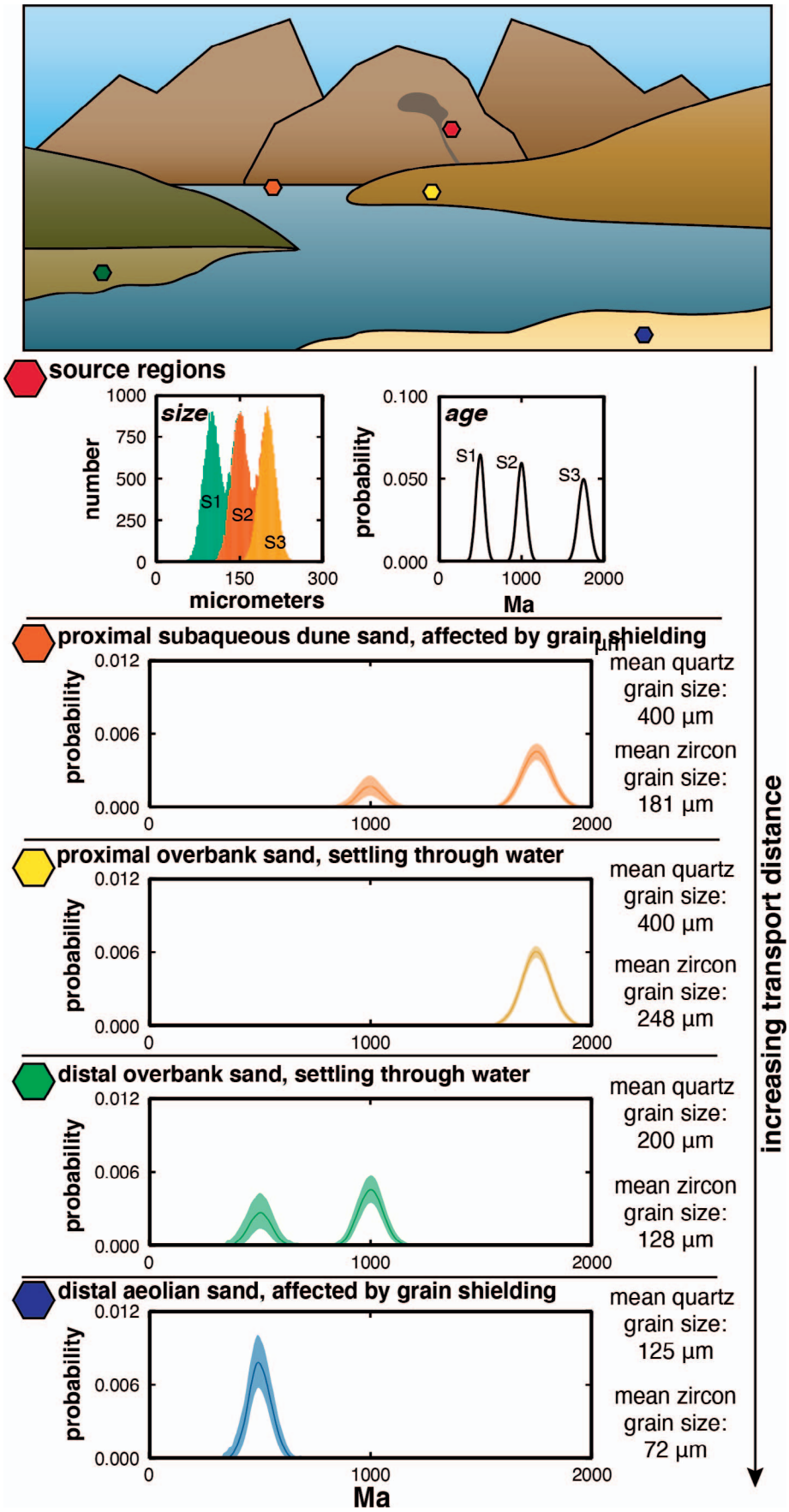

FIG. 6.—Potential detrital-zircon provenance records along a transport path illustrates the combined effect of grain size and settling or selective entrainment on detrital-zircon spectra. The colored hexagons in the landscape illustration correspond to age spectra shown below. The sources panel show three distinct zircon sources, sources 1, 2, and 3, each with a characteristic age and size distribution. Other panels show spectra (95% confidence interval) that correspond to different parts of the sediment transport path. Quartz grain sizes are user-defined and decline with increasing transport distance. Corresponding zircon sizes are determined using the corresponding equations given in the Supplement. Detrital-zircon grain size in overbank sands is modeled using the equations for settling equivalence. Detrital-zircon grain size in proximal, water-laid sands influenced by grain shielding is modeled using the equation of Garzanti et al. (2009) with the density of water. Detrital-zircon grain size in distal, air-laid sands influenced by grain shielding is modeled using the equation of Garzanti et al. (2009) with the density of air. Subsampling of all zircons in this model proceeds as in Figure 5. This model illustrates the possible differential impact of grain size and settling or selective entrainment on detrital-zircon provenance records in systems where detrital-zircon grain size and age systematically co-vary. Despite their different provenance spectra, all samples shown here have identical provenance.

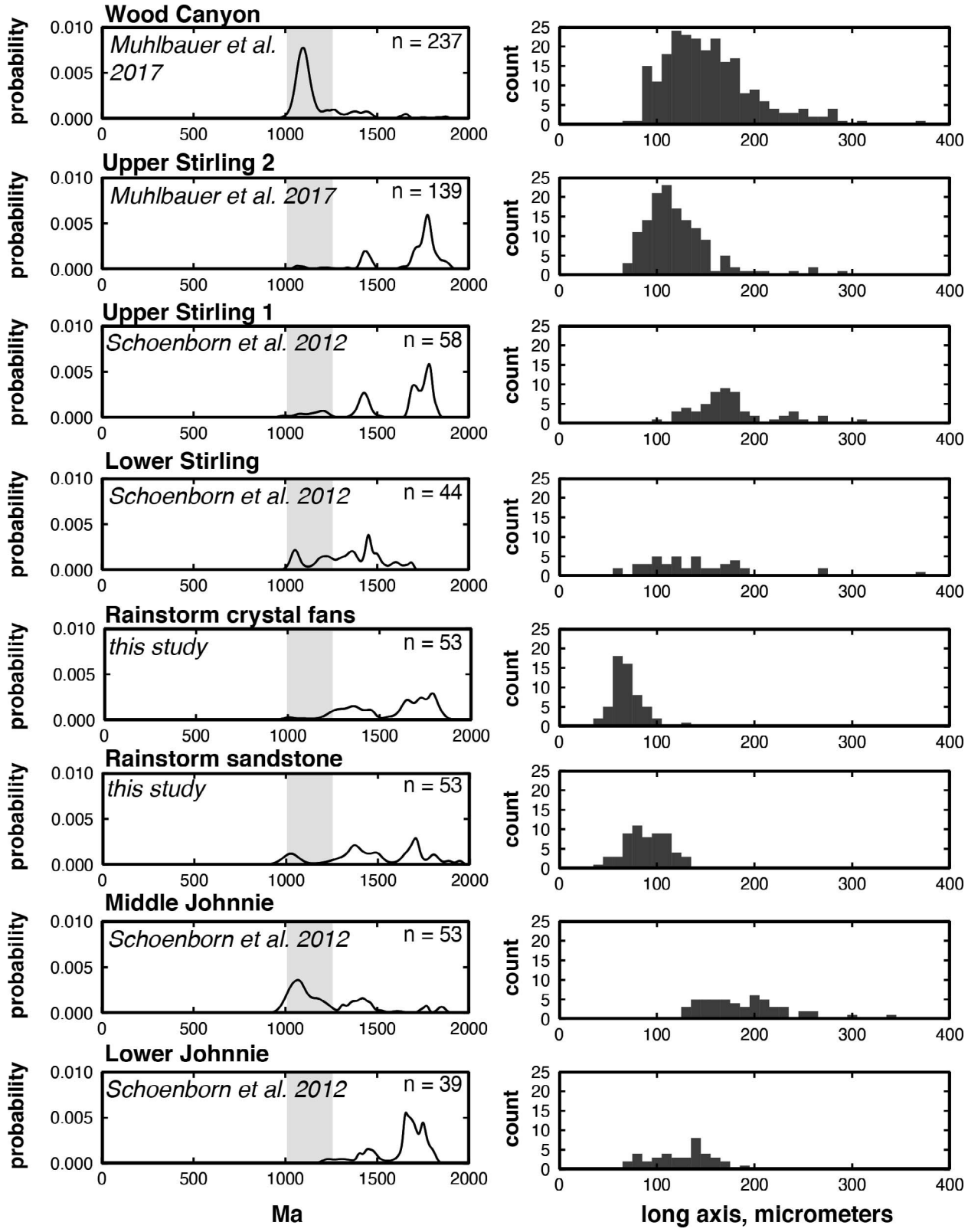

FIG. 7.—Measured age spectra and size distributions for samples included in this study. Grenville age (1.0–1.2 Ga) ranges are highlighted in gray. Samples from the Rainstorm Member are finer grained than other samples.

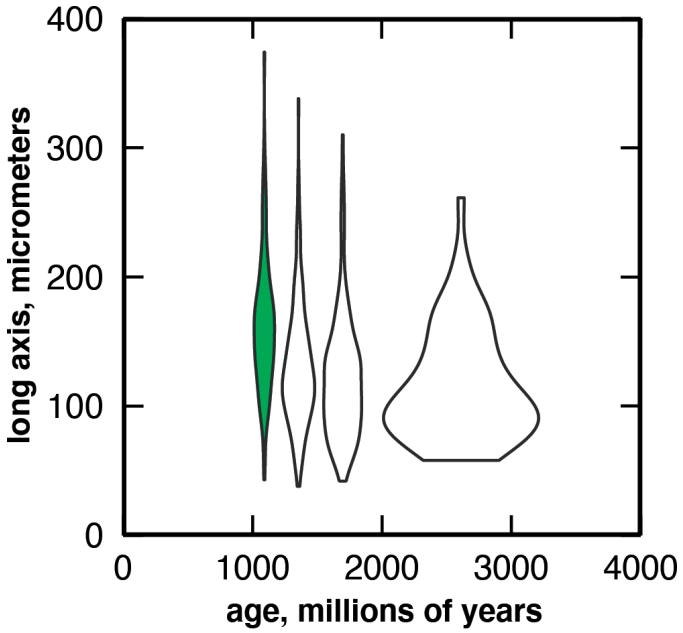

FIG. 8.—Size variation within and between age populations from detrital zircons measured by this study and others (Schoenborn et al. 2012; Muhlbauer et al. 2017). Grenville-age grains (1.0–1.2 Ga, highlighted in green) are larger on average than their older counterparts, though all age populations contain larger and small grains.

samples (Fig. 7). To assess if the detrital-zircon population resulted from size–age fractionation, we split all measured detrital zircons into four size groups based on the length of their major axis (silt, very fine sand, fine sand, and medium sand) (Malusà et al. 2013; Malusà and Garzanti 2019). We calculated empirical cumulative distribution functions of these four size groups (Fig. 9A), plotted their spectra by grain size (Fig. 9B), and assessed the null hypothesis that these size groups were drawn from the same age distribution, using the D-value of the Kolmogorov–Smirnov method (Table 3; see discussion of dissimilarity measures for detrital-zircon geochronology in Vermeesch (2018) and Nordsvan et al. (2020); D-values for all samples are available in the supplement).

This analysis supports the hypothesis that grain size exerts control on the age spectra of these samples. Both the silt and very fine sand grains have a different age distribution in comparison to fine and medium sand grains, though silt and very fine sand grains have a similar distribution, as do fine and medium sand grains. The Kolmogorov-Smirnov D-values also support this conclusion (Table 3). These results highlight the potential role for grain size in creating statistically distinct zircon populations.

Characterization of Crystal-Fan-Associated Clastics.—The clastic residue from dissolution of Rainstorm crystal fans is unusual: most of the sediment, by both volume and mass, was separated into the heavy fraction during heavy-liquid separation using methylene iodide (Table 2). A more typical split between the heavy and light fractions of a sedimentary sandstone would be on the order of 1%.

The density of the light fraction ($\rho = 2.62$ g/cm^3) is similar to that of quartz ($\rho = 2.65$ g/cm^3) and feldspar minerals ($\rho = 2.55$ to 2.78 g/cm^3). The density of the heavy fraction ($\rho = 3.19$ g/cm^3) is slightly less than that of methylene iodide ($\rho = 3.32$ g/cm^3), the heavy liquid used to separate the

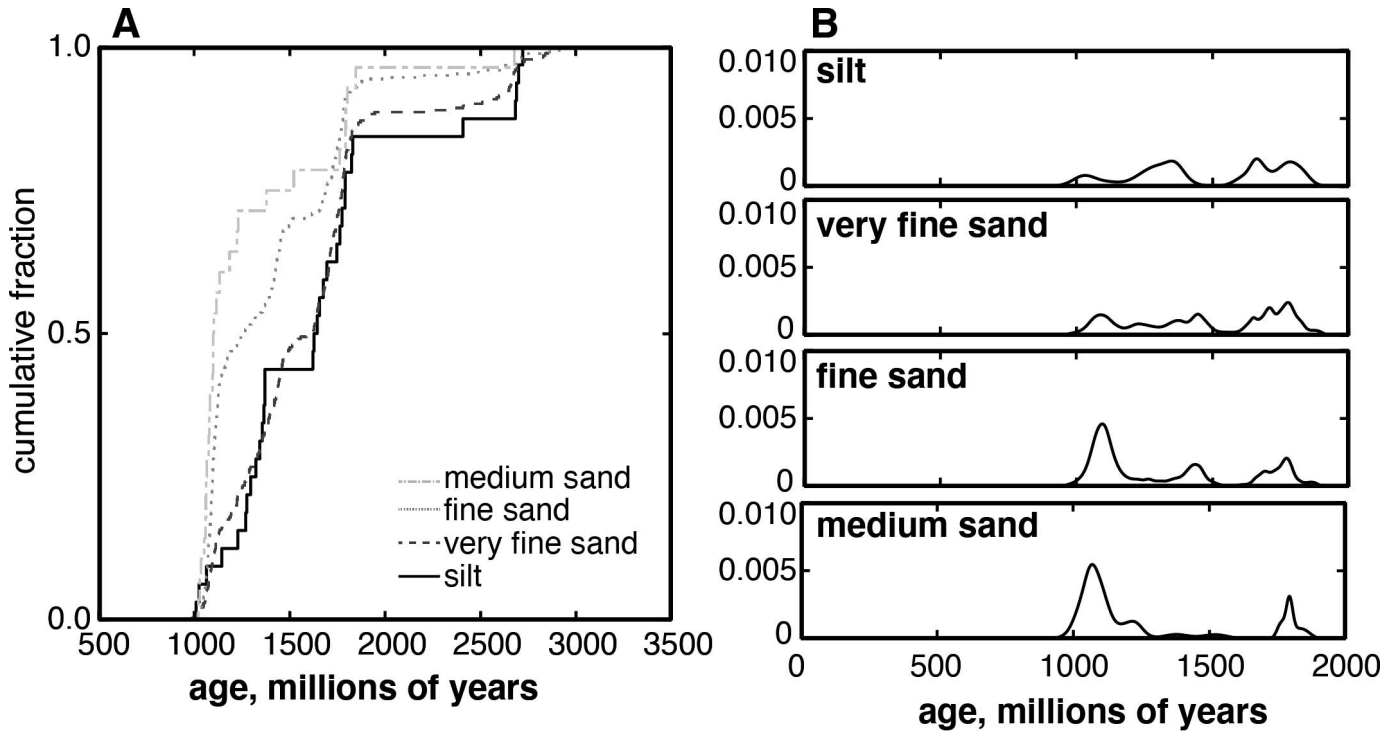

FIG. 9.—These empirical cumulative distribution function curves describe the fraction of grains and their ages in a detrital-zircon dataset measured by this study and others (Schoenborn et al. 2012; Muhlbauer et al. 2017). The silt and very fine sand-size grain populations are similar to each other, as are the fine- and medium-sand-size populations. The largest difference is for Grenville-age (1.0–1.2 Ga) grains, which make up more than 50% of the fine- and medium-sand-size grains but less than 50% of the silt and very fine-sand-size grains.

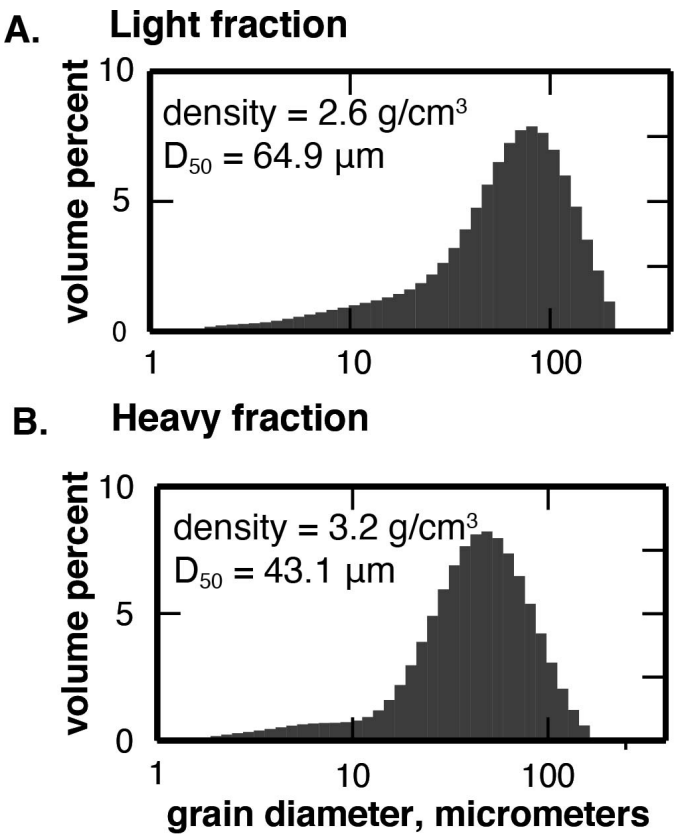

FIG. 10.—LPSA data for both the light and heavy fractions of crystal fan-associated clastic residue are shown.

detrital minerals. The methylene iodide, which had been previously used and recycled in a mineral separation laboratory, may have been incompletely reclaimed following mixing with ethanol, so that it was less dense than expected. Alternate explanations could include grain–grain interactions during settling leading to clumping, with some light grains sinking to the bottom, or air in the pore spaces of sediment during displacement with water.

Grain-size data of intermediate axes measured via LPSA (Table 4, Fig. 10) show that the heavy fraction D_{50} grain size (43.1 μm) is much finer than the light fraction D_{50} grain size (64.9 μm). The predicted sizes of heavy grains, based on the four scenarios outlined above (Fig. 5) (equal sizes, grain shielding, setting through air, and settling through water) and the measured density of the heavy fraction, were compared (Table 4), along with the difference between these calculated grain sizes and the measured grain size. The heavy-fraction D_{50} grain size is closest to the grain-shielding case quantified from observations of a modern aeolian sand (Garzanti et al. 2008), but is even finer.

Modeling Size-Age Relationships in the Ediacaran–Terreneuvian Death Valley Succession

As the grain size of the modeled deposit increases, the relative size and contribution of Grenville-age grains to the resulting spectra also increase (Fig. 11). At a depositional grain-size range of 69 ± 16 μm, between 2% and 20% (95% confidence interval) of the total spectra came from Grenville-age (between 1 and 1.2 Ga) sources. The total-crystal-fan spectra show that 5% of the Grenville-age grains fall in this confidence interval (Fig. S3). At a modeled depositional grain size range of 154 ± 50 μm, between 20% and 55% (95% confidence interval) of the total spectra came from Grenville-age sources. The Wood Canyon Formation spectrum shows that 72% of the grains come from Grenville-age sources, well outside the 95% confidence interval identified here (Fig. S3).

DISCUSSION

Model results highlight that deposition of detrital zircon does not fully describe deposition of other minerals. Such decoupling has been observed between quartz and zircon in an ancient basin (Augustsson et al. 2019). Provenance interpretation based on a single mineral is thus likely to be incomplete. The relative abundance of zircon from different source regions in a sample may not accurately describe the provenance of quartz grains in the same sample. In natural systems, the influences of processes vary in time and space. For example, Steidtmann and Haywood (1982) document oscillations between sediment deposited by airfall and sediment deposited in traction in aeolian strata, as revealed by the changing size relationship of quartz and heavy-mineral grains. A single environment may contain sediment deposited by settling through fluid, traction transport, or mass wasting. These different processes can lead to different biases in provenance records based on measurements of those heavy minerals, like zircon. Additional care is thus warranted in interpreting provenance records, with careful attention to both the average grain size of a sediment sample and of its component detrital zircons.

Analysis of modern rivers suggests that the presence of an age population, rather than the number of grains from that population, is more significant for the interpretation of detrital-zircon spectra (Link et al. 2005). Model results supports this conclusion, suggesting that differences in grain size may affect the proportion of a particular population in a deposit without necessarily requiring a change in the interpretation of provenance. This model also provides a framework for exploring the causes and consequences of such decoupling through settling and selective entrainment.

The Ediacaran–Terreneuvian Succession of Death Valley

Detrital-Zircon Size.—The age spectra of zircons from this succession may have been shaped, in part, by grain size-dependent processes (Fig. 9, Table 4). Across all grains considered here, Grenville-age grains are the largest on average (median long axis size of 160 μm). Other detrital zircon grains are somewhat smaller (median long axis size of 122 μm for grains between 1.2 and 1.5 Ga and 112.7 μm for grains between 1.5 and 1.9 Ga) and the oldest grains (older than 1.9 Ga) have the smallest median long axis size in the dataset (103.2 μm) (Fig. 8). There is substantial overlap in sizes between these age ranges. Large and small zircons occur in each age bin, and the age of an individual grain cannot be derived from its size alone. However, an overall trend of average grain size decreasing with grain age is apparent. This trend is observed outside Laurentia, too (Lawrence et al. 2011; Yang et al. 2012).

One possibility for the pattern mentioned above is that older zircon grains have been subject to more sedimentary cycles of erosion and abrasion, resulting in a smaller average size. Another explanation is that zircon size has varied temporally through Earth history. Geochemical evidence suggests that both Zr concentrations in Earth's continental igneous rocks and overall zircon abundance have increased (Keller et al. 2017). If zircon size scales with Zr concentration and zircon abundance, then temporal variation in average igneous zircon size could result. Limited available grain-size data for zircon grains across Earth history makes further assessment of this hypothesis challenging.

Grenville Sources.—Grenville-age grains are large relative to other detrital zircons in our dataset (Fig. 8). This is consistent with reports that Grenville zircons are large (Moecher and Samson 2006). Observations that Grenville rocks in particular, and igneous rocks connected to the assembly

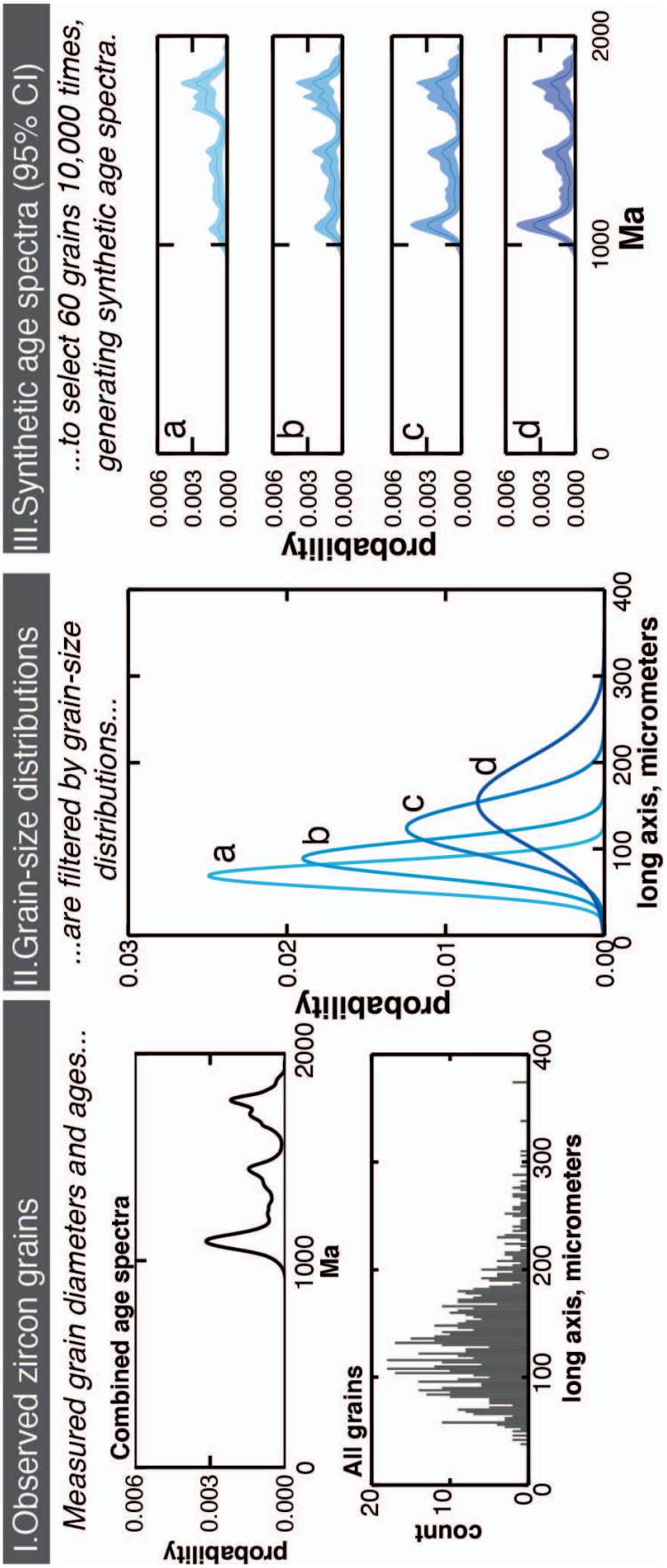

FIG. 11.—All measured concordant zircon grains with a known size from this study and others (Schoenborn et al. 2012; Muhlbauer et al. 2017) are shown in Column I. These grains are pooled together and 60 grains are chosen 10,000 times to generate a series of synthetic age spectra. The grains are selected used size-based probability distribution functions shown in Column II. The 95% confidence interval of the resulting synthetic age spectra are shown in Column III. As the synthetic samples grow coarser (from a to d), the prominence of the Grenville-age peak also grows.

of Rodinia in general, are Zr-rich (Liu et al. 2017; Samson et al. 2018) suggest a likely link between zircon size, abundance, and Zr concentration. As simulated spectra are generated for coarser and coarser samples, the relative contribution and/or the size of the peak associated with Grenville-age sources increases (Fig. 11). To some degree, changing grain size, rather than any change in sediment provenance, may be responsible for differences in the proportion of Grenville-age zircons in a sample. This is perhaps best illustrated by the relatively fine-grained Rainstorm crystal-fan zircons, which were deposited during a period of maximum flooding. This unit has a very minor Grenville-age peak and is the finest and most distal samples studied, consistent with our hypothesis that, in this system, Grenville zircon abundance would decrease with decreasing grain size and increasing transport distance.

Although the lack of a prominent Grenville-age peak in these samples may also reflect a paucity of Grenville-age sources, this is not required by the data. Synthetic spectra generated from the full dataset will also have minor to absent Grenville-age peaks if the synthetic sample has a small grain size (Fig. 11). These results are consistent with Nd isotope analyses by Schoenborn et al. (2012), which suggest a Yavapai–Matzatzal source for the Rainstorm Member but cannot exclude a cryptic Grenville source. As in that study, our detrital-zircon age data do not rule out a Grenville source that may not be represented in the detrital-zircon record because of grain-size effects. The minor Grenville-aged peaks in the two samples taken just above and below the Rainstorm crystal fans, combined with the potential for a "missing" Grenville peak in the Rainstorm crystal fans due to grain-size effects, suggest that Grenville sources could have persisted through the interval.

Muhlbauer et al. (2017) found no evidence that grain-size sorting exerted a strong control on the presence of the prominent Grenville-age peak in the Wood Canyon Formation. The Wood Canyon Fm zircons are the coarsest population examined in this study. None of these synthetic spectra—even the coarsest, which has the same mean grain size and standard deviation as the Wood Canyon Formation sample—contains a Grenville-age peak as large as actually observed. Thus, although grain size may contribute to the substantial Grenville-age peak seen in the Wood Canyon Formation, grain size alone does not account for it. Grain size alone is also unlikely to account for the minimal or absent Grenville-age peaks in the upper Stirling Quartzite or lowermost Johnnie Formation spectra; synthetic spectra coarser than 100 μm have clear Grenville-age peaks (Fig. 11). These data support the conclusion that these stratigraphic shifts may represent genuine shifts in provenance (Schoenborn et al. 2012; Muhlbauer et al. 2017).

These results support the idea that changes in detrital-zircon spectra cannot be *prima facie* evidence for changes in provenance (Lawrence et al. 2011; Ibañez-Mejia et al. 2018). Gaps or peaks in detrital-zircon age spectra may result from a change in provenance, a shift in grain size, and/or a shift in sedimentary processes. Considering both age and grain size together can bolster the case for real changes in provenance or provide alternative interpretations of a detrital record. Expanded datasets that describe the variation of zircon grain size within and between source regions will allow sedimentary geologists to identify source regions and depositional settings in which size must be considered carefully.

Process and Provenance in Rainstorm Member Crystal Fans.—The Rainstorm Member strata and associated sampled zircons are finer than other units in this succession, which is consistent with Rainstorm Member deposition during an interval of maximum flooding (Summa 1993; Bergmann et al. 2011, 2013). The measured grain-size offsets between the heavy and light detrital fractions of Rainstorm crystal strata are puzzling (Table 4). The heavy fraction is finer than the fine fraction—but much finer than would be predicted by any of our scenarios, suggesting that selective entrainment in the Rainstorm yielded a more extreme size shift. Entrainment equivalence between mineral grains has been expressed as a function of grain size, mineral and fluid density, shape, grain stacking geometry, and bed roughness (Komar 2007), although the relationship remains largely empirically untested.

The subaqueous depositional setting of the Rainstorm Member and resulting greater density contrast between heavy and light minerals compared to subaerial settings may have contributed to this large size shift. Rapid carbonate cementation of detrital mineral grains could have led to selective entrainment. Early cementation would impact smaller grains, regardless of their density, to a greater degree than larger grains. Carbonate cementation of siliciclastic deposits is ubiquitous through the Rainstorm Member (Summa 1993). In a study of small asymmetric scours in hummocky cross-stratification in the Rainstorm Member, Summa (1993) suggested that a high degree of sediment cohesion, potentially generated by carbonate cementation, was required to allow the high-angle scour walls, indicating that cementation occurred rapidly following deposition.

The enrichment in heavy minerals in these deposits is also consistent with winnowing of sediment and removal of low-density grains by selective entrainment, which has been observed in modern settings to result in heavy-mineral-rich placer sand (Woolsey et al. 1975; Komar and Wang 1984), consistent with other work on the origin of these deposits (Bergmann et al. 2013). The Rainstorm Member contains hummocky cross-stratification, as well as abundant edgewise conglomerate. Both are interpreted as evidence for high-energy storm events (Summa 1993; Pruss et al. 2008; Bergmann et al. 2013); such events commonly rework sediment. Heavy-mineral grains occur as inter-blade fills (Fig. 4) (Summa 1993; Pruss et al. 2008; Bergmann et al. 2013), and possibly flow baffling by centimeter-scale crystal fans led to the deposition of winnowed, heavy-mineral-rich sediment in the interstices, much as in gravel beds in some modern placer deposits (Slingerland and Smith 1986; Day and Fletcher 1991). These three factors—rapid cementation, winnowing of sediment, and, to some degree, sediment baffling—may all have controlled the presence of small zircon grains in the crystal fan-bearing beds, leading to a minimal Grenville-age peak.

Previous workers suggested that winnowed aeolian sand was as a possible source for the heavy-mineral-rich silt-size siliciclastic sediment in Rainstorm Member marine crystal fans because of their grain size, mineralogy, and depositional style (Bergmann et al. 2013). The winnowing of light minerals by wind from beach dunes is implicated in the formation of some modern beach placer deposits (Woolsey et al. 1975) and storm mobilization of such nearshore sand could have transported sand offshore. However, the size and density of these mineral grains do not conform with predictions for grains settling through air (Table 4) (Bagheri and Bonadonna 2016; Raffaele et al. 2020) although sedimentological evidence indicates extensive, storm-influenced reworking of Rainstorm sediment (Summa 1993; Pruss et al. 2008; Bergmann et al. 2013). Because the interplay between grain size and density reflects sediment's most recent environment (Hand 1967), any earlier aeolian influence could be overprinted following reworking in a subaqueous environment. These data neither rule out, nor require, an aeolian influence on clastic material in the Rainstorm Member.

Sample Number and Grain Size.—Biases in detrital-zircon records related to random sampling and small sample sizes have long been discussed (Andersen 2005). Although studies using smaller sample numbers are commonplace, faster analysis and concerns regarding statistical rigor have motivated the community to work towards larger sample sizes (500–1000 grains) to fully characterize samples (Ibañez-Mejia et al. 2018). Previous provenance work in the Death Valley succession has included smaller zircon populations (e.g., Schoenborn et al. 2012 have sample sizes of less than 62 grains; Stewart et al. 2001 has 2 samples of 22 grains each; Muhlbauer et al. 2017 has the largest sample population from a single unit, n = 237). Rainstorm Member zircons (n = 117) indicate provenance (Fig. 7) consistent with Nd isotope data

(Schoenborn et al. 2012). The Wood Canyon zircon population reported by Muhlbauer et al. (2017) (n = 237) is much larger than that reported by Stewart et al. (2001) (two samples of n = 22 each), and both have similar spectra with a strong, sharp Grenville peak. These observations are both consistent with the suggestion that those smaller-number samples characterize provenance reasonably well in these strata, although not as robustly as larger samples would.

It seems unlikely that analysis of more zircons would meaningfully change the size distribution sampled; detrital grain size likely takes fewer grains to fully characterize than provenance, because depositional processes establish a size range with an upper and lower bound.

CONCLUSION

We find evidence that selective entrainment had a significant effect on the relative contribution of Grenville-age (1.0–1.2 Ga) zircon grains in the detrital zircon record of the Rainstorm Member of the Johnnie Formation. The density and size of detrital grains in beds enriched in heavy minerals in carbonate strata of the Rainstorm Member are consistent with selective entrainment and winnowing of sediment, commonly during storms. The peaks present within the Rainstorm age spectra can be understood as controlled, in part, by transport processes, and perhaps also dynamics of carbonate precipitation. Sedimentological evidence for frequent and energetic storm activity indicates active sediment reworking during deposition of the unit (Summa 1993; Pruss et al. 2008).

Drawing on insights from process-oriented sedimentology, we demonstrate that sediment settling through fluid and selective entrainment may lead to distinct biases in detrital-zircon records. Recognition that detrital zircon grains are not perfect records of provenance, but transported grains subject to sedimentary processes, encourages greater care in interpretations of provenance. A lack of large-scale data regarding how and if zircon size varies through space and time makes it difficult to say conclusively in what scenarios, locations, or time periods grain size might play a key role in shaping detrital-zircon provenance records. However, we suggest that the large size of Grenville-age grains should be considered in other analyses of Laurentian deposits.

ACKNOWLEDGMENTS

We thank S. Maclennan, S. Pruss, B. Schoene, M. Chia, and D. Jones for assistance in the field and/or laboratory, and C. Keinitz for lodging. A.H. Knoll, J.T. Perron, D. McGee, and E. Trower gave feedback on a draft of this manuscript as members of the lead author's thesis committee. Thank you to J.G. Muhlbauer, who provided additional data on grain size-age relationships previously published in Muhlbauer et al. (2017). M.D.C. was funded by a National Defense Science and Engineering Graduate Fellowship. K.D.B. received support from the Packard Foundation. Thanks to Gerilyn Soreghan and Mehrdad Sardar Abadi at the University of Oklahoma for assistance running LPSA samples. The authors thank Associate Editor Paul Myrow, Brandon McElroy, and an anonymous reviewer for their comments and suggestions, and Corresponding Editor John Southard for proofreading.

SUPPLEMENTAL DATA

All data and code related to this project are available at https://github.com/mcantine/rainstorm-zircons and from the SEPM Data Archive: https://www.sepm.org/supplemental-materials.

REFERENCES

Abolins, M., Oskin, R., Prave, T., Summa, C., and Corsetti, F., 2000, Neoproterozoic glacial record in the Death Valley region, California and Nevada: Geological Society of America, Field Guides, v. 2, p. 319–336, doi:10.1130/0-8137-0002-7.319.

Andersen, T., 2005, Detrital zircons as tracers of sedimentary provenance: limiting conditions from statistics and numerical simulation: Chemical Geology, v. 216, p. 249–270, doi:10.1016/j.chemgeo.2004.11.013.

Augustsson, C., Voigt, T., Bernhart, K., Kreißler, M., Gaupp, R., Gärtner, A., Hofmann, M., and Linnemann, U., 2018, Zircon size–age sorting and source-area effect: the German Triassic Buntsandstein Group: Sedimentary Geology, v. 375, p. 218–231, doi:10.1016/j.sedgeo.2017.11.004.

Augustsson, C., Aehnelt, M., Voigt, T., Kunkel, C., Meyer, M., and Schellhorn, F., 2019, Quartz and zircon decoupling in sandstone: petrography and quartz cathodoluminescence of the Early Triassic continental Buntsandstein Group in Germany: Sedimentology, v. 66, p. 2874–2893, doi:10.1111/sed.12620.

Bagheri, G., and Bonadonna, C., 2016, On the drag of freely falling non-spherical particles: Powder Technology, v. 301, p. 526–544, doi:10.1016/j.powtec.2016.06.015.

Bergmann, K.D., Zentmyer, R.A., and Fischer, W.W., 2011, The stratigraphic expression of a large negative carbon isotope excursion from the Ediacaran Johnnie Formation, Death Valley: Precambrian Research, v. 188, p. 45–56, doi:10.1016/j.precamres.2011.03.014.

Bergmann, K.D., Grotzinger, J.P., and Fischer, W.W., 2013, Biological influences on seafloor carbonate precipitation: Palaios, v. 28, p. 99–115, doi:10.2110/palo.2012.p12-088r.

Blum, M.D., Milliken, K.T., Pecha, M.A., Snedden, J.W., Frederick, B.C., and Galloway, W.E., 2017, Detrital-zircon records of Cenomanian, Paleocene, and Oligocene Gulf of Mexico drainage integration and sediment routing: implications for scales of basin-floor fans: Geosphere, v. 13, p. 2169–2205, doi:10.1130/GES01410.1.

Brady, L.L., and Jobson, H.E., 1973, An Experimental Study of Heavy-Mineral Segregation Under Alluvial-Flow Conditions, in Sediment Transport in Alluvial Channels: U.S. Geological Survey, Professional Paper 562, 46 p.

Briggs, L.I., 1965, Heavy mineral correlations and provenances: Journal of Sedimentary Petrology, v. 35, p. 939–955.

Canfield, D.E., Knoll, A.H., Poulton, S.W., Narbonne, G.M., and Dunning, G.R., 2020, Carbon isotopes in clastic rocks and the Neoproterozoic carbon cycle: American Journal of Science, v. 320, p. 97–124, doi:10.2475/02.2020.01.

Carroll, D., 1953, Weatherability of zircon: Journal of Sedimentary Petrology, v. 23, p. 106–116, doi:10.1306/D4269562-2B26-11D7-8648000102C1865D.

Cawood, P.A., Hawkesworth, C.J., and Dhuime, B., 2012, Detrital zircon record and tectonic setting: Geology, v. 40, p. 875–878, doi:10.1130/G32945.1.

Cawood, P.A., Hawkesworth, C.J., and Dhuime, B., 2013, The continental record and the generation of continental crust: Geological Society of America, Bulletin, v. 125, p. 14–32, doi:10.1130/B30722.1.

Cheng, N.-S., 1997, Simplified settling velocity formula for sediment particle: Journal of Hydraulic Engineering, v. 123, p. 149–152.

Chew, D., O'Sullivan, G., Caracciolo, L., Mark, C., and Tyrrell, S., 2020, Sourcing the sand: accessory mineral fertility, analytical and other biases in detrital U-Pb provenance analysis: Earth-Science Reviews, v. 202, no. 103093, doi:10.1016/j.earscirev.2020.103093.

Christie-Blick, N., and Levy, M., 1989, Late Proterozoic and Cambrian tectonics, sedimentation, and record of metazoan radiation in the western United States: Pocatello, Idaho, to Reno, Nevada: American Geophysical Union, Field Trip Guidebook, p. 23–37, doi:10.1029/FT331.

Clapham, M.E., and Corsetti, F.A., 2005, Deep valley incision in the terminal Neoproterozoic (Ediacaran) Johnnie Formation, eastern California, USA: tectonically or glacially driven?: Precambrian Research, v. 141, p. 154–164, doi:10.1016/j.precamres.2005.09.002.

Clift, R., and Gauvin, W.H., 1971, Motion of entrained particles in gas streams: the Canadian Journal of Chemical Engineering, v. 49, p. 439–448, doi:10.1002/cjce.5450490403.

Clifton, H.E., 1969, Beach lamination: nature and origin: Marine Geology, v. 7, p. 553–559, doi:10.1016/0025-3227(69)90023-1.

Corsetti, F.A., and Hagadorn, J.W., 2000, Precambrian–Cambrian transition: Death Valley, United States: Geology, v. 28, p. 299–302, doi:10.1130/0091-7613(2000)028<0299:PCTDVU>2.3.CO;2.

Corsetti, F.A., and Kaufman, A.J., 2003, Stratigraphic investigations of carbon isotope anomalies and Neoproterozoic ice ages in Death Valley, California: Geological Society of America, Bulletin, v. 115, p. 916–932, doi:10.1130/B25066.1.

Corsetti, F.A., Lorentz, N.J., and Pruss, S.B., 2004, Formerly-aragonite seafloor fans from Neoproterozoic strata, Death Valley and southeastern Idaho, United States: implications for "cap carbonate" formation and Snowball Earth: Geophysical Monograph Series, v. 146, p. 33–44, doi:10.1029/146GM04.

Day, S.J., and Fletcher, W.K., 1989, Effects of valley and local channel morphology on the distribution of gold in stream sediments from Harris Creek, British Columbia, Canada: Journal of Geochemical Exploration, v. 32, p. 1–16, doi:10.1016/0375-6742(89)90040-X.

Day, S.J., and Fletcher, W.K., 1991, Accumulation of high-density minerals in pavement voids formation of gravel pavement: Journal of Sedimentary Petrology, v. 61, p. 871–882.

Dickinson, W.R., 2008, Impact of differential zircon fertility of granitoid basement rocks in North America on age populations of detrital zircons and implications for granite petrogenesis: Earth and Planetary Science Letters, v. 275, p. 80–92, doi:10.1016/j.epsl.2008.08.003.

Dickinson, W.R., and Gehrels, G.E., 2009, U-Pb ages of detrital zircons in Jurassic eolian and associated sandstones of the Colorado Plateau: evidence for transcontinental

dispersal and intraregional recycling of sediment: Geological Society of America, Bulletin, v. 121, p. 408–433, doi:10.1130/B26406.1.

Dietrich, W.E., 1982, Settling velocity of natural particles: Water Resources Research, v. 18, p. 1615–1626, doi:10.1029/WR018i006p01615.

Emery, K.O., and Stevenson, R.E., 1950, Laminated beach sand: Journal of Sedimentary Petrology, v. 20, p. 220–223.

Fedo, C.M., and Cooper, J.D., 2001, Sedimentology and sequence stratigraphy of Neoproterozoic and Cambrian units across a craton-margin hinge zone, southeastern California, and implications for the early evolution of the Cordilleran margin: Sedimentary Geology, v. 141–142, p. 501–522, doi:10.1016/S0037-0738(01)00088-4.

Fedo, C.M., Sircombe, K.N., and Rainbird, R.H., 2003, Detrital zircon analysis of the sedimentary record: Reviews in Mineralogy and Geochemistry, v. 53, p. 277–303, doi:10.2113/0530277.

Ferguson, R.I., and Church, M., 2004, A simple universal equation for grain settling velocity: Journal of Sedimentary Research, v. 74, p. 933–937, doi:10.1306/051204740933.

Ferguson, R., Hoey, T., Wathen, S., and Werritty, A., 1996, Field evidence for rapid downstream fining of river gravels through selective transport: Geology, v. 24, p. 179–182, doi:10.1130/0091-7613(1996)024<0179:FEFRDF>2.3.CO;2.

Flowerdew, M.J., Fleming, E.J., Morton, A.C., Frei, D., Chew, D.M., and Daly, J.S., 2020, Assessing mineral fertility and bias in sedimentary provenance studies: examples from the Barents Shelf, *in* Dowey, P., Osborne, M., and Volk, H., eds., Application of Analytical Techniques to Petroleum Systems: Geological Society of London, Special Publication 484, p. 255–274, doi:10.1144/SP484.11.

Friedman, G.M., 1961, Distinction between dune, beach, and river sands from their textural characteristics: Journal of Sedimentary Petrology, v. 31, p. 514–529.

Garzanti, E., Andò, S., and Vezzoli, G., 2008, Settling equivalence of detrital minerals and grain-size dependence of sediment composition: Earth and Planetary Science Letters, v. 273, p. 138–151, doi:10.1016/j.epsl.2008.06.020.

Garzanti, E., Andò, S., and Vezzoli, G., 2009, Grain-size dependence of sediment composition and environmental bias in provenance studies: Earth and Planetary Science Letters, v. 277, p. 422–432, doi:10.1016/j.epsl.2008.11.007.

Gasparini, N.M., Tucker, G.E., and Bras, R.L., 1999, Downstream fining through selective particle sorting in an equilibrium drainage network: Geology, v. 27, p. 1079–1082, doi:10.1130/0091-7613(1999)027<1079:DFTSPS>2.3.CO;2.

Gehrels, G.E., 2000, Introduction to detrital zircon studies of Paleozoic and Triassic strata in western Nevada and northern California, in Paleozoic and Triassic paleogeography and tectonics of western Nevada and Northern California: Geological Society of America, Special Paper 347, p. 1–17, doi:10.1130/0-8137-2347-7.1.

Gehrels, G., 2014, Detrital zircon U-Pb geochronology applied to tectonics: Annual Review of Earth and Planetary Sciences, v. 42, p. 127–149, doi:10.1146/annurev-earth-050212-124012.

Gibbs, R.J., Matthews, M.D., and Link, D.A., 1971, The relationship between sphere size and settling velocity: Journal of Sedimentary Petrology, v. 41, p. 7–18, doi:10.1017/CBO9781107415324.004.

Grigg, N.S., and Rathbun, R.E., 1965, Hydraulic equivalence of minerals with a consideration of the reentrainment process: U.S. Geological Survey, Professional Paper 650, p. 77–80.

Grotzinger, J.P., Fike, D.A., and Fischer, W.W., 2011, Enigmatic origin of the largest-known carbon isotope excursion in Earth's history: Nature Geoscience, v. 4, p. 285–292, doi:10.1038/ngeo1138.

Guo, R., Hu, X., Garzanti, E., Lai, W., Yan, B., and Mark, C., 2020, How faithfully do the geochronological and geochemical signatures of detrital zircon, titanite, rutile and monazite record magmatic and metamorphic events? A case study from the Himalaya and Tibet: Earth-Science Reviews, v. 201, no. 103082, doi:10.1016/j.earscirev.2020.103082.

Hand, B.M., 1967, Differentiation of beach and dune sands, using settling velocities of light and heavy minerals: Journal of Sedimentary Petrology, v. 37, p. 514–520, doi:10.1306/74D71703-2B21-11D7-8648000102C1865D.

Hawkesworth, C.J., Cawood, P.A., Kemp, T., Storey, C., and Dhuime, B., 2009, A matter of preservation: Science, v. 323, p. 49–50.

Hietpas, J., Samson, S., and Moecher, D., 2011a, A direct comparison of the ages of detrital monazite versus detrital zircon in Appalachian foreland basin sandstones: searching for the record of Phanerozoic orogenic events: Earth and Planetary Science Letters, v. 310, p. 488–497, doi:10.1016/j.epsl.2011.08.033.

Hietpas, J., Samson, S., Moecher, D., and Chakraborty, S., 2011b, Enhancing tectonic and provenance information from detrital zircon studies: assessing terrane-scale sampling and grain-scale characterization: Geological Society of London, Journal, v. 168, p. 309–318, doi:10.1144/0016-76492009-163.

Ibañez-Mejia, M., Pullen, A., Pepper, M., Urbani, F., Ghoshal, G., and Ibañez-Mejia, J.C., 2018, Use and abuse of detrital zircon U-Pb geochronology: a case from the Río Orinoco delta, eastern Venezuela: Geology, v. 46, p. 1019–1022, doi:10.1130/G45596.1.

Kaufman, A.J., Corsetti, F.A., and Varni, M.A., 2007, The effect of rising atmospheric oxygen on carbon and sulfur isotope anomalies in the Neoproterozoic Johnnie Formation, Death Valley, USA: Chemical Geology, v. 237, p. 65–81, doi:10.1016/j.chemgeo.2006.06.023.

Keller, C.B., Boehnke, P., and Schoene, B., 2017, Temporal variation in relative zircon abundance throughout Earth history: Geochemical Perspectives Letters, v. 3, p. 179–189, doi:10.7185/geochemlet.1721.

Kodama, Y., 1994, previous studies of abrasion on downstream fining purpose of this study: Journal of Sedimentary Research, v. 64, p. 68–75.

Komar, P.D., 2007, The entrainment, transport and sorting of heavy minerals by waves and currents, developments in sedimentology, *in* Mange, M.E., and Wright, D.T., eds., Heavy Minerals in Use: Elsevier, v. 58, p. 3–48, doi:10.1016/S0070-4571(07)58001-5.

Komar, P.D., and Li, Z., 1988, Applications of grain-pivoting and sliding analyses to selective entrapment of gravel and to flow-competence evaluations: Sedimentology, v. 35, p. 681–695, doi:10.1111/j.1365-3091.1988.tb01244.x.

Komar, P.D., and Wang, C., 1984, Processes of selective grain transport and the formation of placers on beaches: Journal of Geology, v. 92, p. 637–655, doi:10.1086/628903.

Komar, P.D., Clemens, K.E., Li, Z., and Shih, S.M., 1989, The effects of selective sorting on factor analyses of heavy-mineral assemblages: Journal of Sedimentary Petrology, v. 59, p. 590–596, doi:10.1306/212f8ff8-2b24-11d7-8648000102c1865d.

Lawrence, R.L., Cox, R., Mapes, R.W., and Coleman, D.S., 2011, Hydrodynamic fractionation of zircon age populations: Geological Society of America, Bulletin, v. 123, p. 295–305, doi:10.1130/B30151.1.

Leary, R.J., Smith, M.E., and Umhoefer, P., 2020, Grain-size control on detrital zircon cycloprovenance in the late Paleozoic Paradox and Eagle basins, USA: Journal of Geophysical Research, Solid Earth, v. 125, p. 1–19, doi:10.1029/2019JB019226.

Lewin, J., and Brewer, P.A., 2002, Laboratory simulation of clast abrasion: Earth Surface Processes and Landforms, v. 27, p. 145–164, doi:10.1002/esp.306.

Link, P.K., Fanning, C.M., and Beranek, L.P., 2005, Reliability and longitudinal change of detrital-zircon age spectra in the Snake River system, Idaho and Wyoming: an example of reproducing the bumpy barcode: Sedimentary Geology, v. 182, p. 101–142, doi:10.1016/j.sedgeo.2005.07.012.

Liu, C., Knoll, A.H., and Hazen, R.M., 2017, Geochemical and mineralogical evidence that Rodinian assembly was unique: Nature Communications, v. 8, p. 1–7, doi:10.1038/s41467-017-02095-x.

Lowright, R., Williams, E.G., and Dachille, F., 1972, An analysis of factors controlling deviations in hydraulic equivalence in some modern sands: Journal of Sedimentary Petrology, v. 42, p. 635–645, doi:10.1306/74d725e5-2b21-11d7-8648000102c1865d.

Ludwig, K.R., 2003, User's Manual for Isoplot 3.00: A Geochronological Toolkit for Microsoft Excel: Berkeley Geochronology Center Special Publication.

Mackey, G.N., Horton, B.K., and Milliken, K.L., 2012, Provenance of the Paleocene-Eocene Wilcox Group, western Gulf of Mexico basin: evidence for integrated drainage of the southern Laramide Rocky Mountains and Cordilleran arc: Geological Society of America, Bulletin, v. 124, p. 1007–1024, doi:10.1130/B30458.1.

Malkowski, M.A., Sharman, G.R., Johnstone, S.A., Grove, M.J., Kimbrough, D.L., and Graham, S.A., 2019, Dilution and propagation of provenance trends in sand and mud: geochemistry and detrital zircon geochronology of modern sediment from central California (U.S.A.): American Journal of Science, v. 319, p. 846–902, doi:10.2475/10.2019.02.

Malusà, M.G., and Garzanti, E., 2019, The sedimentology of detrital thermochronology, *in* Malusà, M.G., and Fitzgerald, P.G., eds., Fission-Track Thermochronology and Its Application to Geology: Springer, p. 123–143.

Malusà, M.G., Carter, A., Limoncelli, M., Villa, I.M., and Garzanti, E., 2013, Bias in detrital zircon geochronology and thermochronometry: Chemical Geology, v. 359, p. 90–107, doi:10.1016/j.chemgeo.2013.09.016.

Malusà, M.G., Resentini, A., and Garzanti, E., 2016, Hydraulic sorting and mineral fertility bias in detrital geochronology: Gondwana Research, v. 31, p. 1–19, doi:10.1016/j.gr.2015.09.002.

Matthews, J.J., Liu, A.G., Yang, C., McIlroy, D., Levell, B., and Condon, D.J., 2020, A chronostratigraphic framework for the rise of the Ediacaran macrobiota: new constraints from Mistaken Point Ecological Reserve, Newfoundland: Geological Society of America, Bulletin, p. 1–13, doi:10.1130/b35646.1.

McIntyre, D.D., 1959, The hydraulic equivalence and size distributions of some mineral grains from a beach: The Journal of Geology, v. 67, p. 278–301.

McQuivey, R.S., and Keefer, T.N., 1969, The relation of turbulence to the deposition of magnetite over ripples: U.S. Geological Survey, Professional Paper 650-D, p. 244–247.

Minguez, D., Kodama, K.P., and Hillhouse, J.W., 2015, Paleomagnetic and cyclostratigraphic constraints on the synchroneity and duration of the Shuram carbon isotope excursion, Johnnie Formation, Death Valley Region, CA: Precambrian Research, v. 266, p. 395–408, doi:10.1016/j.precamres.2015.05.033.

Moecher, D.P., and Samson, S.D., 2006, Differential zircon fertility of source terranes and natural bias in the detrital zircon record: implications for sedimentary provenance analysis: Earth and Planetary Science Letters, v. 247, p. 252–266, doi:10.1016/j.epsl.2006.04.035.

Moecher, D.P., Kelly, E.A., Hietpas, J., and Samson, S.D., 2019, Proof of recycling in clastic sedimentary systems from textural analysis and geochronology of detrital monazite: implications for detrital mineral provenance analysis: Geological Society of America, Bulletin, v. 131, p. 1115–1132, doi:10.1130/B31947.1.

Morton, A.C., and Hallsworth, C., 2007, Stability of detrital heavy minerals during burial diagenesis, *in* Mange, M.A., and Wright, D.T., eds., Heavy Minerals in Use: Elsevier, Developments in Sedimentology, v. 58, p. 215–245, doi:10.1016/S0070-4571(07)58007-6.

Muhlbauer, J.G., Fedo, C.M., and Farmer, G.L., 2017, Influence of textural parameters on detrital-zircon age spectra with application to provenance and paleogeography during the Ediacaran–Terreneuvian of southwestern Laurentia: Geological Society of America, Bulletin, v. 129, p. 1595–1601, doi:10.1130/B31611.1.

Nordsvan, A.R., Kirscher, U., Kirkland, C.L., Barham, M., and Brennan, D.T., 2020, Resampling (detrital) zircon age distributions for accurate multidimensional scaling solutions: Earth-Science Reviews, v. 204, no. 103149, doi:10.1016/j.earscirev.2020.103149.

Paola, C., Parker, G., Seal, R., Sinha, S.K., Southard, J.B., and Wilcock, P.R., 1992, Downstream fining by selective deposition in a laboratory flume: Science, v. 258, p. 1757–1760.

Petterson, R., Prave, A.R., Wernicke, B.P., and Fallick, A.E., 2011, The Neoproterozoic Noonday Formation, Death Valley region, California: Geological Society of America, Bulletin, v. 123, p. 1317–1336, doi:10.1130/B30281.1.

Prave, A.R., 1999, Two diamictites, two cap carbonates, two $\delta^{13}C$ excursions, two rifts: the Neoproterozoic Kingston Peak Formation, Death Valley, California: Geology, v. 27, p. 339–342.

Pruss, S.B., Corsetti, F.A., and Fischer, W.W., 2008, Seafloor-precipitated carbonate fans in the Neoproterozoic Rainstorm Member, Johnnie Formation, Death Valley Region, USA: Sedimentary Geology, v. 207, p. 34–40, doi:10.1016/j.sedgeo.2008.03.005.

Raffaele, L., Bruno, L., and Sherman, D.J., 2020, Statistical characterization of sedimentation velocity of natural particles: Aeolian Research, v. 44, no. 100593, doi:10.1016/j.aeolia.2020.100593.

Rittenhouse, G., 1943, Transportation and deposition of heavy minerals: Geological Society of America, Bulletin, v. 54, p. 1725–1780.

Rooney, A.D., Cantine, M.D., Bergmann, K.D., Gómez-Pérez, I., Al Baloushi, B., Boag, T.H., Busch, J.F., Sperling, E.A., and Strauss, J.V., 2020, Calibrating the coevolution of Ediacaran life and environment: National Academy of Sciences (USA), Proceedings, v. 117, p. 16, 824–16,830, doi:10.1073/pnas.2002918117.

Rubey, W.W., 1933, Settling velocity of gravel, sand, and silt particles: American Journal of Science, v. 25, p. 325–338, doi:10.2475/ajs.s5-25.148.325.

Sallenger, A.H., 1979, Inverse grading and hydraulic equivalence in grain flow deposits: Journal of Sedimentary Petrology, v. 49, p. 553–562, doi:10.1306/212F7789-2B24-11D7-8648000102C1865D.

Samson, S.D., Moecher, D.P., and Satkoski, A.M., 2018, Inherited, enriched, heated, or recycled? Examining potential causes of Earth's most zircon fertile magmatic episode: Lithos, v. 314–315, p. 350–359, doi:10.1016/j.lithos.2018.06.015.

Schoenborn, W.A., 2010, Geochemistry of the Neoproterozoic Johnnie Formation and Stirling Quartzite, Southern Nopah Range, California: Deciphering the Roles of Climate, Tectonics, and Sedimentary Process in Reconstructing the Early Evolution of a Rifted Continental Margin [Ph.D. Thesis]: George Washington University, 322 p.

Schoenborn, W.A., Fedo, C.M., and Farmer, G.L., 2012, Provenance of the Neoproterozoic Johnnie Formation and Stirling Quartzite, southeastern California, determined by detrital zircon geochronology and Nd isotope geochemistry: Precambrian Research, v. 206–207, p. 182–199, doi:10.1016/j.precamres.2012.02.017.

Slama, J., and Kosler, J., 2012, Effects of sampling and mineral separation on accuracy of detrital zircon studies: Geochemistry, Geophysics, Geosystems, v. 13, p. 1–17, doi:10.1029/2012GC004106.

Slingerland, R.L., 1977, The effects of entrainment on the hydraulic equivalence relationships of light and heavy minerals in sands: Journal of Sedimentary Petrology, v. 47, p. 753–770, doi:10.1306/212f7243-2b24-11d7-8648000102c1865d.

Slingerland, R., 1984, Role of hydraulic sorting in the origin of fluvial placers: Journal of Sedimentary Petrology, v. 54, p. 137–150, doi:10.1306/212F83C8-2B24-11D7-8648000102C1865D.

Slingerland, R., and Smith, N.D., 1986, Occurrence and formation of water-laid placers: Annual Review of Earth and Planetary Sciences, v. 14, p. 113–147.

Smith, N.D., and Beukes, N.J., 1983, Bar to bank flow convergence zones: a contribution to the origin of alluvial placers: Economic Geology, v. 78, p. 1342–1349, doi:10.2113/gsecongeo.78.7.1342.

Smithson, F., 1950, The mineralogy of arenaceous deposits: Science Progress, v. 149, p. 10–21.

Spencer, C.J., Kirkland, C.L., and Roberts, N.M.W., 2018, Implications of erosion and bedrock composition on zircon fertility: examples from South America and Western Australia: Terra Nova, v. 30, p. 289–295, doi:10.1111/ter.12338.

Steidtmann, J.A., and Haywood, H.C., 1982, Settling velocities of quartz and tourmaline in eolian sandstone strata: Journal of Sedimentary Petrology, v. 52, p. 395–399, doi:10.1306/212f7f63-2b24-11d7-8648000102c1865d.

Stevens, T., Palk, C., Carter, A., Lu, H., and Clift, P.D., 2010, Assessing the provenance of loess and desert sediments in northern China using U-Pb dating and morphology of detrital zircons: Geological Society of America, Bulletin, v. 122, p. 1331–1344, doi:10.1130/B30102.1.

Stewart, J.H., 1970, Upper Precambrian and Lower Cambrian Strata in the Southern Great Basin, California and Nevada: U.S. Geological Survey, Professional Paper 620, 206 p.

Stewart, J.H., Gehrels, G.E., Barth, A.P., Link, P.K., Christie-Blick, N., and Wrucke, C.T., 2001, Detrital zircon provenance of Mesoproterozoic to Cambrian arenites in the western United States and northwestern Mexico: Geological Society of America, Bulletin, v. 113, p. 1343–1356, doi:10.1130/0016-7606(2001)113<1343:DZPOMT>2.0.CO;2.

Summa, C.L., 1993, Sedimentologic, Stratigraphic, and Tectonic Controls of a Mixed Carbonate–Siliciclastic Succession: Neoproterozoic Johnnie formation, Southeast California [Ph.D. Thesis]: Massachusetts Institute of Technology, 616 p.

Trower, E.J., and Grotzinger, J.P., 2010, Sedimentology, diagenesis, and stratigraphic occurrence of giant ooids in the Ediacaran Rainstorm Member, Johnnie Formation, Death Valley region, California: Precambrian Research, v. 180, p. 113–124, doi:10.1016/j.precamres.2010.03.007.

Verdel, C., Wernicke, B.P., and Bowring, S.A., 2011, The Shuram and subsequent Ediacaran carbon isotope excursions from southwest Laurentia, and implications for environmental stability during the metazoan radiation: Geological Society of America, Bulletin, v. 123, p. 1539–1559, doi:10.1130/B30369.1.

Vermeesch, P., 2018, Dissimilarity measures in detrital geochronology: Earth-Science Reviews, v. 178, p. 310–321, doi:10.1016/j.earscirev.2017.11.027.

Witkosky, R., and Wernicke, B.P., 2018, Subsidence history of the Ediacaran Johnnie Formation and related strata of southwest Laurentia: implications for the age and duration of the Shuram isotopic excursion and animal evolution: Geosphere, v. 14, p. 2245–2276, doi:10.1130/GES01678.1.

Woolsey, J.R., Henry, V.J., and Hunt, J.L., 1975, Backshore heavy-mineral concentration on Sapelo Island, Georgia: Journal of Sedimentary Petrology, v. 45, p. 280–284, doi:10.1306/212f6d39-2b24-11d7-8648000102c1865d.

Yang, S., Zhang, F., and Wang, Z., 2012, Grain size distribution and age population of detrital zircons from the Changjiang (Yangtze) River system, China: Chemical Geology, v. 296–297, p. 26–38, doi:10.1016/j.chemgeo.2011.12.016.

Received 30 September 2020; accepted 17 June 2021.